Since January 2020 Elsevier has created a COVID-19 resource centre with free information in English and Mandarin on the novel coronavirus COVID-19. The COVID-19 resource centre is hosted on Elsevier Connect, the company's public news and information website.

Cities 135 (2023) 104238

Contents lists available at ScienceDirect

Cities

journal homepage: www.elsevier.com/locate/cities

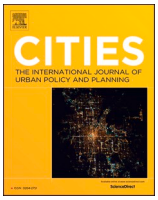

The impact of traffic control measures on the spread of COVID-19 within urban agglomerations based on a modified epidemic model

Wang Xiang [a], Li Chen [a], Xuedong Yan [c], Bin Wang [b], Xiaobing Liu [c,*]

[a] Hunan Key Laboratory of Smart Roadway and Cooperative Vehicle-Infrastructure Systems, Changsha University of Science & Technology, Changsha 410114, China
[b] Alibaba Cloud Computing Co. Ltd., Changsha 410007, China
[c] Key Laboratory of Transport Industry of Big Data Application Technologies for Comprehensive Transport, Beijing Jiaotong University, Beijing 100044, China

ARTICLE INFO

Keywords:
Traffic control measures
COVID-19
Spread mechanism
Epidemic model
Urban agglomeration
Population migration

ABSTRACT

With the spatial structure of urban agglomerations, well-developed transportation networks and close economic ties can increase the risk of intercity transmission of infectious diseases. To reveal the epidemic transmission mechanism in urban agglomerations and to explore the effectiveness of traffic control measures, this study proposes an Urban-Agglomeration-based Epidemic and Mobility Model (UAEMM) based on the reality of urban transportation networks and population mobility factors. Since the model considers the urban population inflow, along with the active intracity population, it can be used to estimate the composition of urban cases. The model was applied to the Chang-Zhu-Tan urban agglomeration, and the results show that the model can better simulate the transmission process of the urban agglomeration for a certain scale of epidemic. The number of cases within the urban agglomeration is higher than the number of cases imported into the urban agglomeration from external cities. The composition of cases in the core cities of the urban agglomeration changes with the adjustment of prevention and control measures. In contrast, the number of cases imported into the secondary cities is consistently greater than the number of cases transmitted within the cities. A traffic control measures discount factor is introduced to simulate the development of the epidemic in the urban agglomeration under the traffic control measures of the first-level response to major public health emergency, traffic blockades in infected areas, and public transportation shutdowns. If none of those traffic control measures had been taken after the outbreak of COVID-19, the number of cases in the urban agglomeration would theoretically have increased to 3879, which is 11.61 times the actual number of cases that occurred. If only one traffic control measure had been used alone, each of the three measures would have reduced the number of cases in the urban agglomeration to 30.19 %–57.44 % of the theoretical values of infection cases, with the best blocking effect coming from the first-level response to major public health emergency. Traffic control measures have a significant effect in interrupting the spread of COVID-19 in urban agglomerations. The methodology and main findings presented in this paper are of general interest and can also be used in studies in other countries for similar purposes to help understand the spread of COVID-19 in urban agglomerations.

1. Introduction

As we all know, we are still combating COVID-19 three years since its emergence (Wang et al., 2022). The COVID-19 epidemic continues to have a significant impact on the livelihood of the population, and the economic development and future of cities is in jeopardy (Hu et al., 2021). According to WHO data, by the end of September 2022, the cumulative number of confirmed cases worldwide exceeded 500 million, with >5.7 million deaths due to COVID-19. Many attempts have been made to block the spread of the epidemic, not only through medical measures, but also through many effective non-pharmacological interventions (Takefuji, 2022; Wang et al., 2022).

The theory behind non-pharmacological interventions is to limit population build-up and movement, and traffic control is the most effective way to do this (Xiang, Chen, Peng, Wang, Liu, 2022a). To block the spread of the epidemic, >140 countries around the world have taken various traffic control measures, including home quarantine, public transport shutdowns and traffic shutdowns in infected areas (Gao et al., 2022; Mayer & Boston, 2022). In the United States, Australia and China, the most common traffic control measures used include shutting down

* Corresponding author.
E-mail address: lxiaobing@bjtu.edu.cn (X. Liu).

https://doi.org/10.1016/j.cities.2023.104238
Received 1 December 2021; Received in revised form 30 December 2022; Accepted 8 February 2023
Available online 13 February 2023

public transportation in cities at the center of the outbreak, blocking all modes of transportation in the infected areas of cities and requiring residents to stay at home in quarantine for about 14 days if there are cases of infection in their community (Beck et al., 2021; Goenaga et al., 2021; S. Lai, Ruktanonchai, Zhou, Prosper, et al., 2020a; Z. Liu & Stern, 2021). In addition, some countries have declared states of emergency in some cities or the whole country to encourage residents to stay in their homes and reduce unnecessary travel, such as New Zealand's "Alert Level System", Japan's "State of Emergency", and China's " first-level response to major public health emergency" (S. Liu & Yamamoto, 2022; Mayer & Boston, 2022). Countries with more severe epidemics have adopted direct measures of total blockades, for example France and India (Dablanc et al., 2022; Pulla, 2020).

As global cities continue to evolve and develop, urban clusters are becoming more and more common (Cantuarias-Villessuzanne et al., 2021), consisting of an urban agglomeration with a large city as the core and two or more supporting cities, forming a compact spatial organization, with close economic ties and highly developed transportation (Kim et al., 2018). This kind of regional spatial structure is common around the world, examples including the Chang-Zhu-Tan and Beijing-Tianjin-Hebei urban agglomerations in China, the Rhine-Ruhr urban agglomeration in Germany, the Seoul urban agglomeration in Korea, and the Greater Paris area in northwestern Europe (da Cruz et al., 2020; Moreno-Monroy et al., 2021; Ohmagari, 2022). The emergence of urban agglomerations provides cities with better opportunities for development, but also imposes new challenges for the prevention and control of public health emergencies such as COVID-19. Urban epidemic prevention and control face many dilemmas (Yonghong Xiao & Torok, 2020). Due to the complex social activities that go on between cities, over-control can affect intercity linkages and development, while measures that are too lax can lead to the further spread of an epidemic between cities (Sajadi & Hartley, 2022). Therefore, reasonable and effective traffic prevention and control for urban agglomerations facing an epidemic must be studied and discussed in today's circumstances.

This study attempts to explore some issues of epidemic prevention and control from an urban agglomeration perspective, by examining the spread of cases between cities. First, we ask what is the composition of cases in each member of the studied urban agglomeration, and how each member can develop prevention and control measures specifically aimed at cases coming from inside and outside of the city. Second, we look at how many cases are being imported from outside of the urban agglomeration members to the urban agglomeration, and how such cases can be prevented and controlled. Third, we ask how cases spread among the members within the urban agglomeration. Fourth, we study the effectiveness of the traffic control measures taken by each member of the urban agglomeration in terms of blocking cases.

To explore the above issues, this paper develops an Urban-Agglomeration-based Epidemic and Mobility Model (UAEMM) capable of simulating urban case composition and intercity case transmission. The improvements compared with the city-based epidemic and mobility model (CEMM) (Wei et al., 2021) include three aspects: (1) the active population within the city is considered in predicting the spread of internal cases; (2) the cure rate is considered; and (3) the distance attenuation effect is considered in cross-city transmission. Then, using the Chang-Zhu-Tan urban agglomeration as a case study, we investigate the case composition of each city, the number of cases imported from non-members of the urban agglomeration cluster to the urban agglomeration and the cross-transmission among urban agglomeration members. Moreover, the effect of traffic control measures taken by urban agglomeration members to block case transmission is quantified. The methods and ideas used in this study can provide valuable reference material for the development of traffic control measures in urban agglomerations.

The rest of the paper is structured as follows: Section 2 provides a literature review, Section 3 the methodology, Section 4 describes the case study and data sources, Section 5 presents the results and analysis, and Section 6 offers a discussion and conclusion.

2. Literature review

Modeling infectious diseases requires complex systems work (Sanz et al., 2014). Since Cohen's work on pioneering models of human infectious diseases, scientists have worked on various mathematical models for studying the spread of infectious diseases (Cohen, 1992). Different infectious diseases have different epidemiological characteristics, and the models built are also highly variable (Li et al., 2021). The major infectious disease models that have been created for COVID-19 can broadly be divided into the following two groups:

The first group contains the classical infectious disease models based on SIR (Susceptible-Infected-Recovered) and SEIR (Susceptible-Exposed-Infected-Recovered) (Kermack & McKendrick, 1939; Lekone & Finkenstädt, 2006; Jielun Liu et al., 2022; Shulgin et al., 1998). These models can be a good fit for urban epidemics, describing quantitatively the development and elimination of an epidemic through indicators such as peak, peak period and basic regeneration number (He et al., 2020; Yang et al., 2020). To determine the effects of different intervention measures on the spread of COVID-19, scholars have varied the SIR and SEIR models by introducing different populations. For example, Nguyen et al. (2022) established the SIR-M model by adding the mobile population M to the SIR model, and used this to study the evolution of the epidemic in Melbourne, Australia, under different prevention and control measures; Liu et al. (2022) then proposed the SEPIR model based on the SEIR model but considering a pre-symptomatic population P. They used their model to evaluate the effects of stay-at-home requirements and travel restrictions on the spread of cases in the Tokyo urban agglomeration; Chuan et al. (2020) added the quarantine population Q to develop the SEQIR model, and used it to evaluate the effectiveness of quarantine measures in India at the time. Other models along similar lines include SEIQRD (Ghostine et al., 2021), SEAHIR (Leontitsis et al., 2021), MSEIR (X. Chen, Zhang, Wang, Gallaher, & Zhu, 2021b) and SEIRD (Maugeri et al., 2020).

The second group comprises the machine learning and deep learning of infectious disease models in the context of big data. Such models have been widely used in the analysis and propagation prediction of COVID-19 (Shorten et al., 2021). Chimmula et al. use LSTM (long short-term memory) models under deep learning to predict the arrival of the Canadian epidemic's turning point; Mphale et al. (Mphale, Okike, & Rafifing, 2022) use a machine-learning time-series model, the autoregressive integrated moving average (ARIMA) model, to predict the 60-day outbreak in Botswana in order to better combat it; Zhang et al. (2020)(Zhang, Ji, Zheng, Ye, & Li, 2020) assess the impact of a city lockdown in limiting the spread of COVID-19, through deep-learning and network science models. Other examples include comparative modeling using six deep-learning time-series methods (Zeroual et al., 2020), modeling using machine learning combined with logistic models (Tian et al., 2020) and modeling using artificial neural networks (Ghanim et al., 2022).

The transmission models proposed in the above studies can offer a good fit for the development of city epidemics and provide a valid assessment of epidemic prevention and control measures. Yet they ignore the characteristics of intercity (or international) transmission of cases, i.e., the relevant spatial aspects of infectious disease transmission are largely ignored (Arino et al., 2007). Studies of urban epidemics usually assume closed rooms, which is clearly unreasonable. Therefore, Wei et al. (Wei et al., 2021) proposed the CEMM based on an urban spatial network perspective to model the spatial spread of cases. However, their intracity case projections were based on the existing number of infected cases and existing transmission rates in the city, rather than on the intensity of citizens' intracity travel, preventing accurate modeling of the structure of cases in the city. Because the COVID-19 virus spreads mainly through human activity, it is often more accurate to predict its transmission chain based on the activity of residents

(Truong & Truong, 2021). In addition, Wei et al. (Wei et al., 2021) were unable to quantify the proportion of cases imported from each city, or to assess either the impact of transportation measures on cases within and outside of the city or the effect of blocking on specific cities from which cases were being imported.

The main contributions of this study are as follows: first, breaking with the traditional notion of the room and board model, a UAEMM is proposed to simulate the spread of cases between cities as well as within cities, based on the realistic context of urban transportation networks and intercity population mobility factors, and considering the active intracity population. Second, since imported cases from distant cities tend to be overestimated, we also consider distance decay effects for inputs from non-members of the urban agglomeration, calibrated by the Gaussian function. Finally, policy factors are introduced and calibrated using a difference in differences (DID) model, and then used to simulate the development pattern under different traffic control measures. The methodology and main findings presented in this paper will be of general interest and can also be used in other countries for similar purposes to help the understanding of the spread of COVID-19 in urban agglomerations.

3. Methodology

3.1. Theoretical basis of the model

Population migration is a factor that cannot be ignored in infectious disease research. It can lead to the transmission of carriers of the virus. Generally speaking, if there is an infected but undiagnosed individual in a city, exhibiting travel behavior, then a certain percentage of people will be infected. The greater the scale of population migration, the more infections there will be. In other words, the scale of population migration between cities represents the probability of the spread of infectious diseases. The spread of infectious diseases can occur not only within cities, considering each city as a specific population, but also from one city to another due to travel. However, existing studies have mainly focused on case spread caused by population export from the cities at the epidemic center to other cities, while case spread in cities that are not epidemic centers has been less studied, and this type of research method can be considered single epidemic center export, as shown in Fig. 1.

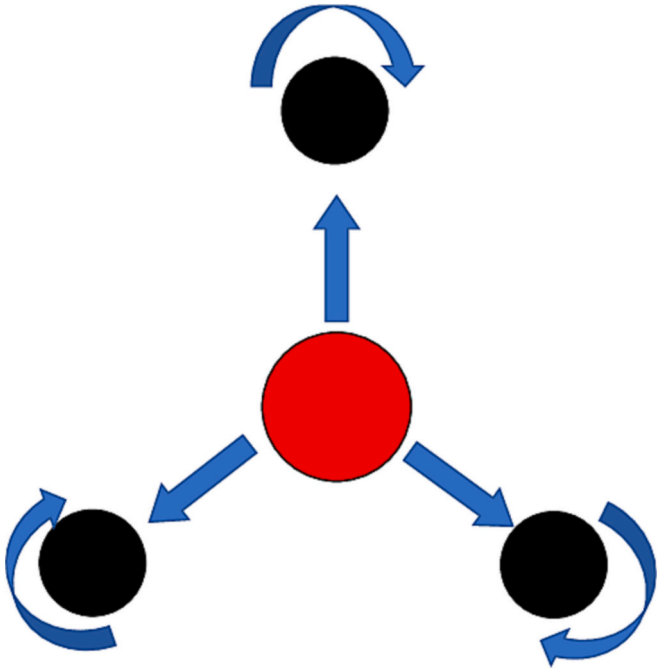

Fig. 1. Single Center Mode.

It should be said that many countries have now formed more complete high-speed transportation networks. China has a relatively well-developed high-speed rail network. Korea, the U.S. and Japan also have very mature rail, air and high-speed rail layouts, and their cities are easily accessible. Further, with the exception of some less developed countries, most countries are linked within a more complete international transportation network. This shows that population flow between cities can occur through various modes of transportation, such as high-speed rail, ordinary railroad, and air. The greater the accessibility of transportation, the easier is the spread of cases. Thus, in a context where populations can migrate rapidly, case spread may not only come from the city that is at the center of the outbreak, but also from other cities or countries. This requires a multi-city epidemic spread model that considers not only the spread of the epidemic from the city at its center, but also the spread from non-central cities, as shown in Fig. 2. Non-coincidentally, 43 % of the early cases reported outside of Wuhan (before January 23, 2020) had no known travel history to Wuhan, and these cases were distributed throughout China. Therefore, this study will use the multi-city epidemic spread model as the basis for constructing its model and conducting the analysis.

3.2. Urban-agglomeration-based epidemic and mobility model

1. The model of migration scale between two cities

The migration scale between two cities is calculated from the total scale of the first city's move-out and the proportion of that migration that goes to the second city, as shown in Eq. (1):

$$\begin{bmatrix} I_{1,1,t} & \cdots & I_{1,j,t} \\ \vdots & \ddots & \vdots \\ I_{i,1,t} & \cdots & I_{i,j,t} \end{bmatrix} = S_{i,t}^{out} \times \begin{bmatrix} \omega_{1,1,t} & \cdots & \omega_{1,j,t} \\ \vdots & \ddots & \vdots \\ \omega_{i,1,t} & \cdots & \omega_{i,j,t} \end{bmatrix} \tag{1}$$

where $S_{i,t}^{out}$ is the total move-out scale of city i at time t; $\omega_{i,j,t}$ is the percentage of city i's move-out that migrates to city j at time t; and $I_{i,j,t}$ is the migration scale between city i and city j at moment t.

2. The model of imported infection cases

There are two important factors to be considered in the spread of intercity case import. First, the spread of cases between cities has a distance attenuation effect. This means that the number of cases far from the center of the outbreak tends to be overestimated and the number close to the center of the outbreak underestimated. Second, returns to scale is the basis for many powerful results in economics and economic geography (Bond-Smith, 2021). Power functions are often used to measure the pattern of increasing or decreasing returns to scale (Szakolczai & Stahl, 1969). The performance of the power function is also usually more important than the performance of other functions when

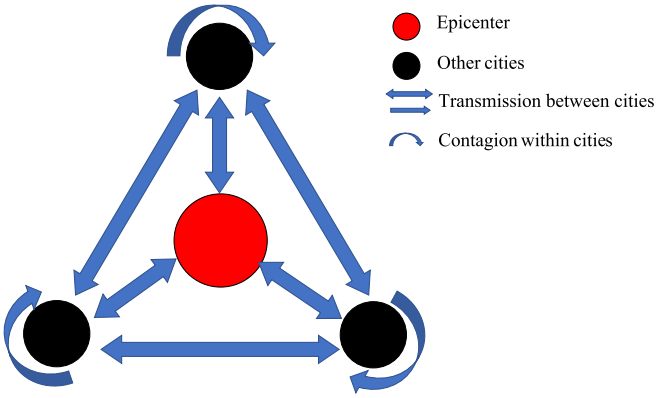

Fig. 2. Multi-city epidemic centered spread mode.

studying population mobility patterns (Schlapfer et al., 2021). Therefore, in this study, the power function was also used to characterize the impact of the decreasing scale effect on population mobility.

Seeing each city as an epidemic center, the characteristics of each city node will include the number of COVID-19 cases, and the scale of the migration between the original city and the destination city. The prediction model of imported cases is as follows:

$$A_{j,t}^{i\rightarrow} = E_{i,t-1} \times \beta \times \left[I_{i,j,t-1} \times G(d_{ij}) \right]^n \quad (2)$$

where $A_{j,t}^{i\rightarrow}$ is the predicted number of infected cases imported from city i to city j at time t; $E_{i,\,t-1}$ is the initial seed, that is the number of cases in city i at time $t-1$, $t-1$means the day before time t. For example, if t represents January 24, then $t-1$ represents January 23; β is the transmission rate, which can be calculated according to the growth in the number of infected cases at the epidemic center; $I_{i,\,j,\,t-1}$ is the migration scale from city i to city j at time $t-1$; $G(d_{ij})$ is the distance decay factor. In addition, through repeated experiments, the best fit between estimated and actual cases was achieved when the value of n was close to $\frac{1}{2}$.This means that when I (the scale of population migration) increases by 1 %, the value of $A_{j,\,t}^{+}$increases by 0.5 %. The introduction of a power function describes the fact that the growth rate of infected cases is lower than the growth rate of the scale of population mobility when cases spread between cities, and also explains the fact that in urban agglomerations the number of cases contracted is much less high than expected, despite the fact that some members have larger population inflows.

3. The model of intracity infection cases

Besides the intercity transmission, COVID-19 also spreads within each city. Therefore, this model considers the amount of intracity travel to establish a prediction model for intracity infections:

$$A_{j,t}^{+} = E_{j,t-1} \times \beta \times \alpha_{j,t-1} \times \theta \quad (3)$$

where $A_{j,\,t}^{+}$is the increase in the number of cases in city j at time t; $E_{j,\,t-1}$ is the initial seed, that is the number of cases in city j at time $t-1$; θ is the epidemic reduction factor, a value ranging from 0 to 1; $\alpha_{j,\,t-1}$ is the amount of travel and migration inside city j at time $t-1$.

4. The model of aggregated infection cases

However, as cases spread, some patients will be cured as the level of diagnosis improves. Therefore, we also consider the cure rate in the model. The total predicted number of infection cases in this city at time t is the sum of the cases at time t-1, minus the cured cases, plus the predicted number of imported cases and the predicted number of intracity cases:

$$A_{j,t} = A_{j,t-1}\left(1-\gamma_{j,t}\right) + \sum_i A_{j,t}^{i\rightarrow} + A_{j,t}^{+} \quad (4)$$

In Eq. (4), $\gamma_{j,\,t}$is the cure rate by city $j$at t, calculated from the number of infection cases and the number of cured cases, and $A_{j,\,t-1}$ is the number of cases diagnosed by city j at $t-1$. $\sum_i A_{j,t}^{i\rightarrow}$ is the sum of the number of cases imported into city from all other cities at moment t.

5. Epidemics under different traffic control measures

In real life, the final control effect is the result of the superposition of multiple policy effects and instruments. Therefore, we add a factor to discount the effect, and name this factor the traffic control policy factor. By adding the traffic control policy factor and quantifying the traffic prevention and control effects of different measures, we have:

$$A_{j,P,t} = \rho_{p,imported} \times A_{j,t}^{i\rightarrow} + \rho_{p,internal} \times A_{j,t}^{+} \quad (5)$$

Where ρ_p is the effect of traffic control policy P on the number of cases. Since different measures have different effects inside and outside the city, we consider both the import effect, $\rho_{p,\,imported}$, and the effect of intracity propagation, $\rho_{p,\mathrm{internal}}$. We established a simple classical DID regression model, based on Baidu migration big data, to find different traffic control policy effects. It is also adjusted to the level of decision making, the impact on traffic, and the degree of policy implementation and disposition for different measures implemented in the existing literature and in real life; $A_{j,\,P,\,t}$ is the number of cases in city j at time t under policy P.

Eqs. (1) to (5) can be unified as the UAEMM, through which the case structure of an urban cluster can be predicted, and the epidemic trend estimated under different traffic control measures. In Table 1, we compare the UAEMM with the CEMM.

Description of parameters in CEMM: $N_{j,\,t}^{i\rightarrow}$ is the number of cases imported from city i to city $j$at time t; $N_{i,\,t-1}$ is the number of cases in city i at time $t-1$; $N_{j,\,t}^{+}$ is the number of additional local cases in city j at time t; $N_{j,\,t}$ is the number of cases in city j at time t.

6. Distance decay effect

In order to simulate the distance decay effect, we introduce the Gaussian function, which is widely used as a distance decay function, as shown in Eq. (6).

$$G(d_{ij}) = \frac{exp\left(-\frac{1}{2}\left(\frac{d_{ij}}{d_0}\right)^2\right) - exp\left(-\frac{1}{2}\right)}{1 - exp\left(-\frac{1}{2}\right)}, d_{ij} \le d_0 \quad (6)$$

Here, $G(d_{ij})$ is the distance decay factor; $d_{i,\,j}$ denotes the geometric distance between cities i and j; $d_0$reflect the geometric distance between the two furthest cities in China.

7. DID model for determining policy factors

To determine the values of the different policy factors ρ_{p}, we build a simple classical DID model for regression estimation, as follows:

$$ln\left(S_{i,t}\right) = \theta_0 + \theta_1 \cdot R_{i,t} + \rho_p \cdot T_{i,t} \cdot R_{i,t} + \theta_3 \cdot T_{i,t} + \varepsilon_{i,t} \quad (7)$$

Here, $\ln(S_{i,\,t})$ is the logarithmic value of the scale of population migration (including out-migration, in-migration and intracity population mobility) in city i during time period t. $T_{i,\,t}$ is a group dummy variable, where 1 indicates the treatment group and 0 the control group. $R_{i,\,t}$ is the policy variable, which equals 1 during the phase of implementing the traffic measures and 0 in other time periods. θ_0 is a constant, θ_1 a policy effect coefficient and θ_3 a treatment group coefficient. ρ_p is the coefficient of the interaction term $T_{i,\,t} \cdot R_{i,\,t}$, which is the quantified

Table 1
UAEMM vs CEMM.

Equations	UAEMM	CEMM	Distinction
Intercity communication	$A_{j,\,t}^{i\rightarrow} = E_{i,\,t-1} \times \beta \times [I_{i,\,j,\,t-1} \times G(d_{ij})]^n$	$N_{j,t}^{i\rightarrow} = \frac{N_{i,t-1} \times \beta \times P_{ij}}{popu_i}$	Distance attenuation factor $G(d_{ij})$ is considered; Decreasing returns to scale n is considered
Intracity dissemination	$A_{j,\,t}^{+} = E_{j,\,t-1} \times \beta \times \alpha_{j,\,t-1} \times \theta$	$N_{j,\,t}^{+} = N_{j,\,t-1} \times \beta \times \theta$	Intracity travel factor $\alpha_{j,\,t-1}$ is considered
Total formula	$A_{j,t} = A_{j,t-1}\left(1-\gamma_{j,t}\right) + \sum_i A_{j,t}^{i\rightarrow} + A_{j,t}^{+}$	$N_{j,t} = N_{j,t-1} + \sum_i N_{j,t}^{i\rightarrow} + N_{j,t}^{+}$	Cure rate γ is considered
Modeling under different traffic control measures	$A_{j,\,P,\,t} = \rho_{p,\,imported} \times A_{j,\,t}^{i\rightarrow} + \rho_{p,\,internal} \times A_{j,\,t}^{+}$	None	

result of the policy effect. $\varepsilon_{i,t}$ is the disturbance term.

8. Epidemic reduction factor and cure rate

The epidemic reduction factor θ shows the degree of severity of the epidemic in the city and the epidemiological risk of cases within the city. In general, if the value of θ is equal to or close to 0, the city is considered to have a low degree of epidemic severity and a low risk of intra-city epidemics; in contrast, a value of θ of 1 or close to 1 is considered to have a high degree of epidemic severity and a higher risk of intra-city epidemics. As shown in Eq. (8).

$$\theta = \frac{E_{i,t}}{\sum_{i=0}^{n} E_{n,t}} \tag{8}$$

All parameters in the equation have the same meaning as in the above. Eq. (8) is defined as the epidemic discount factor and is equal to the ratio of the number of confirmed cases in city i at moment t to the sum of the number of confirmed cases in all cities at moment t.

The cure rate is calculated as shown in Eq. (9).

$$\gamma_{i,t} = \frac{R_{i,t}}{E_{i,t-1}} \tag{9}$$

$R_{i,t}$ is the number of populations cured in city i at time t. Other parameters have the same meaning as in the above.

3.3. Multi-agent system as a technical support

The multi-agent system (MAS) is a multidisciplinary fusion of complex adaptive systems, artificial life and distributed artificial intelligence (Davila et al., 2005). This method can be an important tool for complex system analysis and simulation, and has been widely used in epidemic simulation. In existing multi-agent models, the agents usually represent single units, and the epidemic spread between units takes place through mutual contact. In this study, using cities as the basic unit of analysis, the assumption is that each city is an agent node and the city population scale, number of infection cases and other parameters are used as node characteristics. The amount of migration of populations between cities is considered to be a connection between agent nodes, so that a multi-agent network, also known as an urban network, can be built. Therefore, the spatial spread of the infectious disease (COVID-19) can be simulated as the growth in the number of infection cases in cities and their spread between the cities in an urban network, with Netlogo software used to implement a specific simulation process.

4. Application to the case of the Chang-Zhu-Tan urban agglomeration

4.1. Study area and COVID-19 facts

As aggregations of a number of megalopolises and metropolises, urban agglomerations develop on the basis of frequent population movements. China has already stepped into a new phase of a central city leading the development of an urban agglomeration and then the urban agglomeration driving the development of regional economies (Yao Xiao et al., 2021). A high population density and close regional relations are the most marked characteristics of agglomerations. For example, the three adjacent cities of Changsha, Zhuzhou and Xiangtan in China's Hunan Province share close geographical connections and frequent economic exchanges, while population flow between these three cities

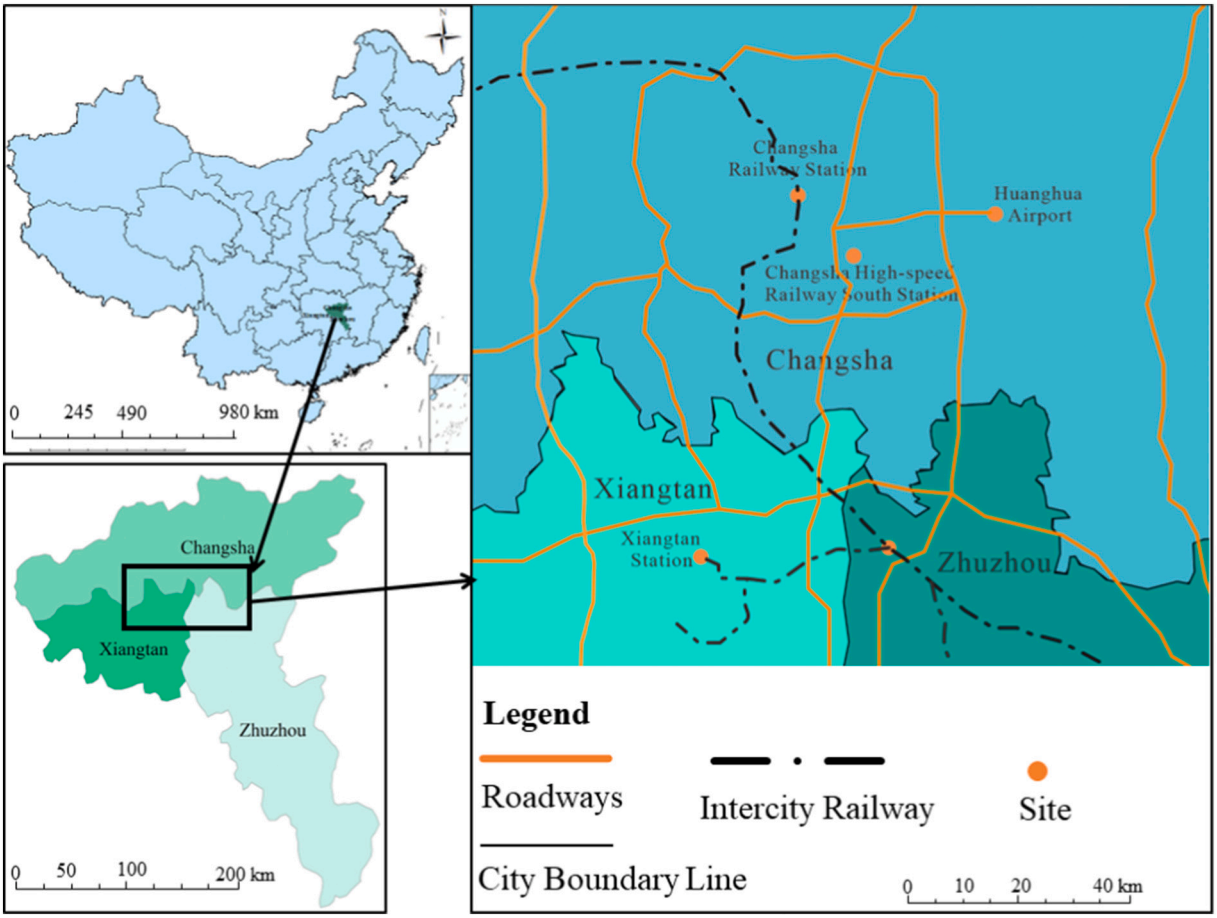

Fig. 3. Location of Chang-Zhu-Tan urban agglomeration in China and its transportation conditions.

accounts for 39.67 % of the total population flow within the entire province.

We chose the Chang-Zhu-Tan urban agglomeration as the application case for this paper. Chang-Zhu-Tan is located in the important Yangtze River Delta economic belt of China (Fig. 3). It currently has a population of 15.30 million, which is 26 % of the total population of Hunan Province. Continually propelled by the integration measures implemented by this agglomeration, these three cities have become increasingly close due to traffic links comprising intercity railways, expressways and national/provincial roads. This has stimulated population migration among the cities, with large amounts of off-site commuting and weekend roundtrips. Five intercity bus routes have already been introduced within the Chang-Zhu-Tan urban agglomeration, while intercity trains have become a form of mass transit, with the number of one-day trains having been increased to 76.5 pairs. The total number of travel interactions in these three cities has reached about 400,000 per day. As a result, population migration has become more flexible and concentrated, while the epidemic's spread has become more threatening. The multi-city interactive transmission model should thus be adopted to simulate an epidemic's spread in an urban agglomeration.

On January 12, 2020, the diagnosis of the first COVID-19 patient in Changsha was confirmed. Due to being the Hunan provincial capital and the closest city of the three to Wuhan, Changsha ended up having the severest epidemic outbreak, with 241 diagnosed cases in total, while Zhuzhou reported 78 and Xiangtan 35 (as shown in Figs. 4 and 5). It can be seen that the peak period of new cases in Changsha was mainly from January 27 to February 7, while the numbers of daily-added cases in Zhuzhou and Xiangtan were both small, and as a result the general epidemic variation was stable in that period. The number of daily-added cases in this agglomeration dropped after February 10.

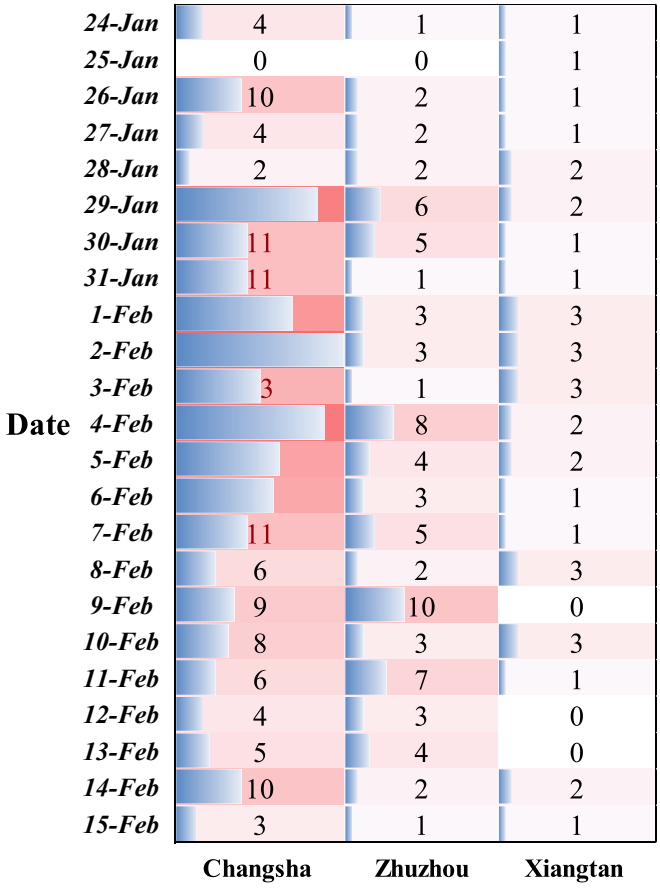

Fig. 4. New daily cases in the Chang-Zhu-Tan urban agglomeration.

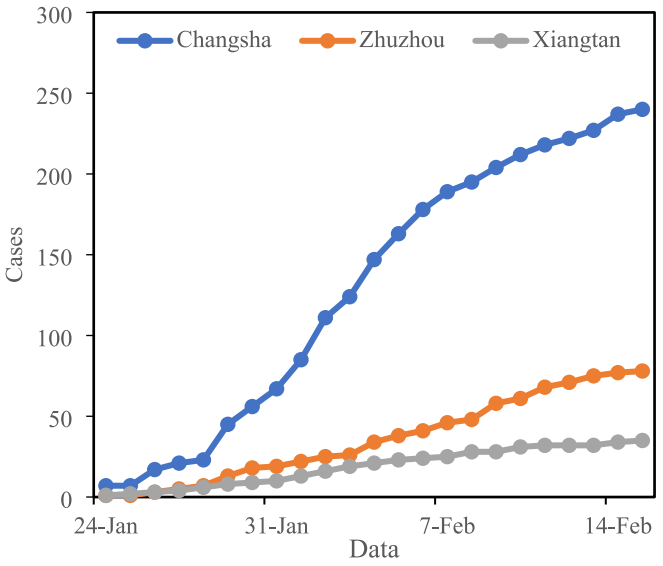

Fig. 5. Trend in number of COVID-19 cases in the Chang-Zhu-Tan urban agglomeration.

4.2. Traffic control measures

At the beginning of the COVID-19 outbreak, three types of policies were commonly formulated by Chinese governments at all levels: firstly, the most severe type was the activation of the level 1 response to public health incidents, by provinces and municipalities directly under the central government, which required the people's governments at all levels to suspend work and schools (H. Chen, Shi, Zhang, Wang, & Sun, 2021a; Kandel et al., 2020). The second type consisted of traffic blockades in the infected areas, so as to strictly control traffic. This strategy was to limit the population outflow from the infected areas and reduce the risk of the spread of the epidemic, which was the most important measure used to contain the spread of the epidemic from the center to the outside. The third type was a passenger transportation shutdown in cities with serious epidemics, used to reduce the possibility of human-to-human contact and thus COVID-19 transmission (Xiang, Chen, Peng, Wang, Liu, 2022b). The three measures, the decision-making levels, the scope of their impact, the impact on traffic, and degree of policy implementation and disposition are shown in Table 2.

Hunan Province and the Chang-Zhu-Tan urban agglomeration also initiated three outbreak prevention and control measures in the early stages of the outbreak, including a first-level response to major public health emergency, a traffic blockade in the infected areas and a public transportation shutdown, aiming to curb the spread of COVID-19 with these traffic control measures. On January 24, after the first case of COVID-19 was confirmed in Hunan Province, the government immediately activated the level 1 response to the public health event, while the prefecture cities of the Chang-Zhu-Tan urban agglomeration subsequently formulated traffic control measures at different time-points. Changsha launched the public health event level 1 response on January 24 before executing traffic controls on public transport and in the epidemic-affected areas. On January 27, Zhuzhou started to implement strict controls on the vehicles moving into and out of Hubei Province, before completely shutting down urban public transport on February 2. Xiangtan exercised epidemic controls for intercity, intracity and public traffic starting from January 28. The time-points and main details of the major traffic control measures implemented in the agglomeration are shown in Fig. 6 below:

4.3. Data source

The population migration data were sourced from the Big Data of

Table 2
Information about the three mainstream measures.

Policy	Decision-making levels	Scope of policy's impact	Impact on traffic	Degree of policy implementation and disposition	Permitted travel and conditions
First-level response to major public health emergency	Provincial government	Provincial scope	All modes of transportation	Ultra strictly	Allowing a family member to shop that needs to be nucleic acid negative; allowing people with serious illnesses to travel for medical treatment; allowing special workers (medical staff, community workers, etc.) who are nucleic acid negative to commute to work.
Traffic blockades in infected areas	Municipal and county governments	Infected areas	All modes of transportation in the infected areas	More strictly	Allow people in non-infected areas to travel for shopping, work, and school as normal if they are nucleic acid negative.
Public transportation shutdown	Municipal and county governments	Intracity and intercity	City buses, subways and cabs and intercity buses	Strictly	Allow cross-city travel for private vehicles with a negative 24-hour nucleic acid test certificate.

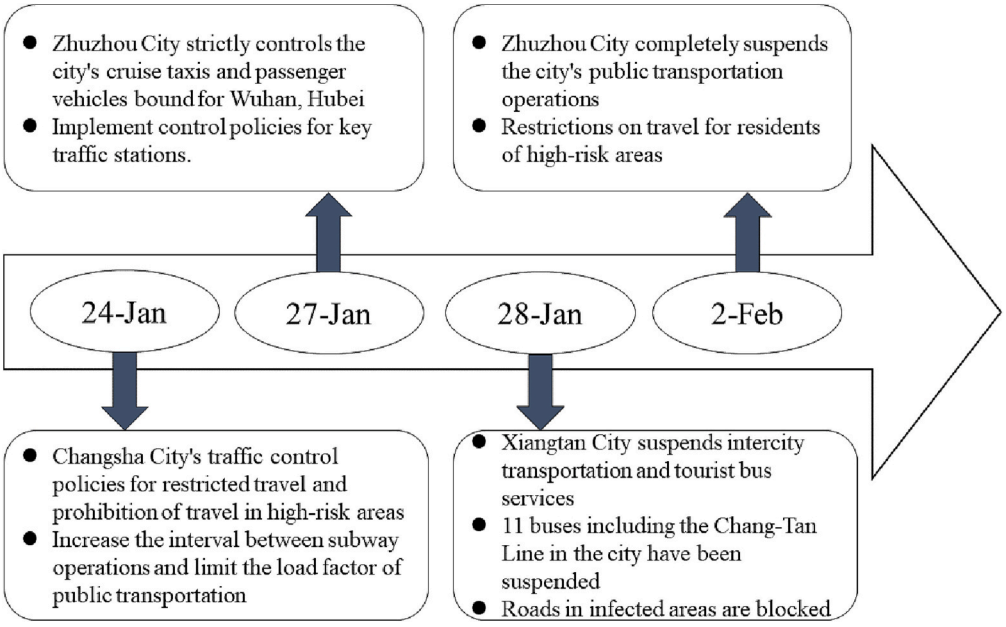

Fig. 6. Time-points of traffic control measures of Chang-Zhu-Tan urban agglomeration.

Baidu Migration (http://qianxi.baidu.com/). Baidu Migration Big Data is calculated using massive amounts of spatial and temporal big data, combined with artificial intelligence technology. The sources include (1) the Baidu Map app; (2) third-party applications that require geolocation services from Baidu Map; (3) an open platform for transportation and travel big data built through a cooperation between Baidu Map and government transportation departments. As of 2020, the Baidu Maps open platform has provided location services for over 500,000 apps, with an average of over 120 billion location service requests per day, and some extremely large-scale mobile phone systems and apps are using the location services. In terms of the breadth of the Baidu migration big data sources, they include the numbers of people using various migration modes such as roads, high-speed rail and air, but do not give the individual numbers migrating using each transportation mode. Against the background of the popularity of smart devices, it has more advanced breadth, accuracy and validity than traditional population census data.

For this study, Baidu migration data were used for the three cities in the Chang-Zhu-Tan agglomeration, from January 1 to February 15, 2020, with the percentage of the migrations from original city to destination city (Fig. 7(a)-(c)), the total move-out scale (Fig. 7(d)), and total amount of intracity travel and migration (Fig. 7(e)). Due to the lack of migration ratio data in 2019, we adopted the migration ratio data from the same period of the lunar calendar in 2021 as a substitute. Based on that, we studied and analyzed the weights of the intercity population migration. According to the UAEMM, imported infection cases and intracity infection cases were fitted into the epidemic data of Chang-Zhu-Tan in 2020. In addition, the numbers of diagnosed COVID-19 cases in the cities of the Chang-Zhu-Tan agglomeration from January 24, 2020 to February 15, 2020 were retrieved from the official data released by the Municipal Health Committee of each city in that period.

5. Results analysis

Before proceeding to the analysis of the results, a special note is needed. In this paper, we consider all cities associated with the Chang-Zhu-Tan urban agglomeration and with a certain scale of epidemic in the simulation process but, due to the space limitations of the paper, we cannot analyze the case interaction between each city and the Chang-Zhu-Tan urban agglomeration. Specifically, we look at the cities outside the urban agglomeration uniformly as an input source, and then analyze the epidemic's spread between the Chang-Zhu-Tan urban agglomeration and the external cities. Reviewing the timeline of the actual COVID-19 outbreak, the overseas outbreaks did not reach a certain scale until March 2020. Therefore, since we study the time period from late January 2020 to mid-February 2020, the importation of overseas cases was not considered.

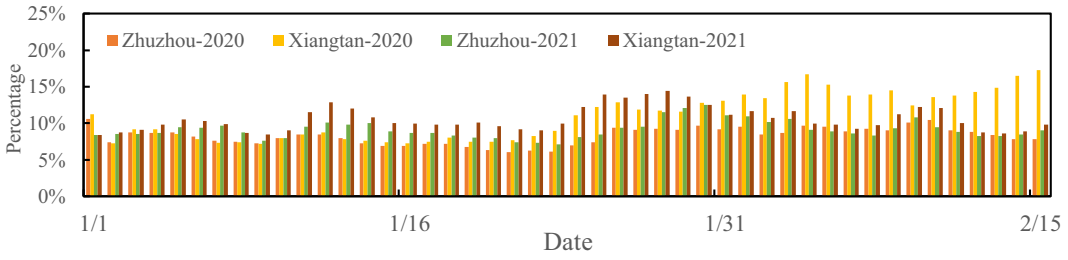

(a). Percentage of Changsha migrating to Zhuzhou and Xiangtan

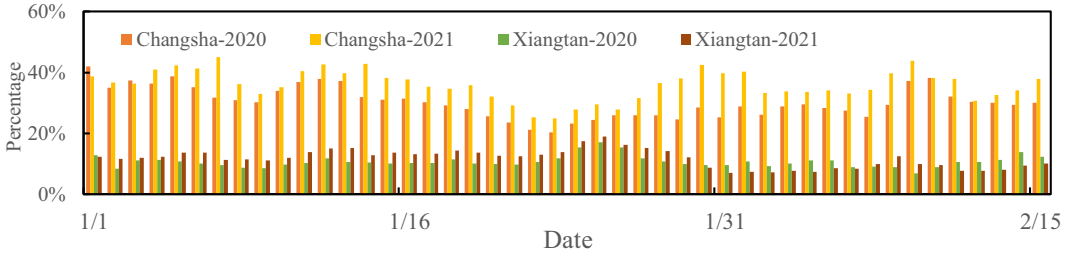

(b). Percentage of Zhuzhou migrating to Changsha and Xiangtan

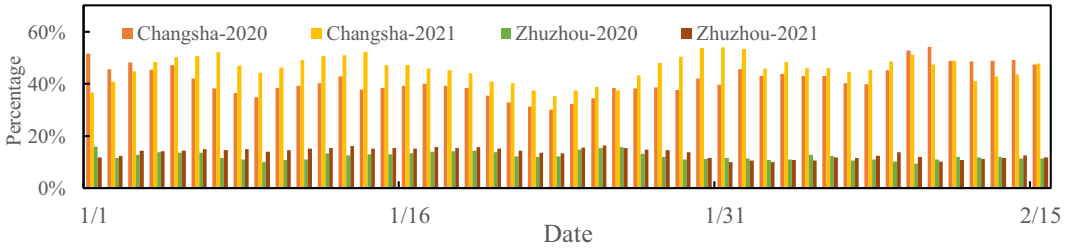

(c). Percentage of Xiangtan migrating to Changsha and Zhuzhou

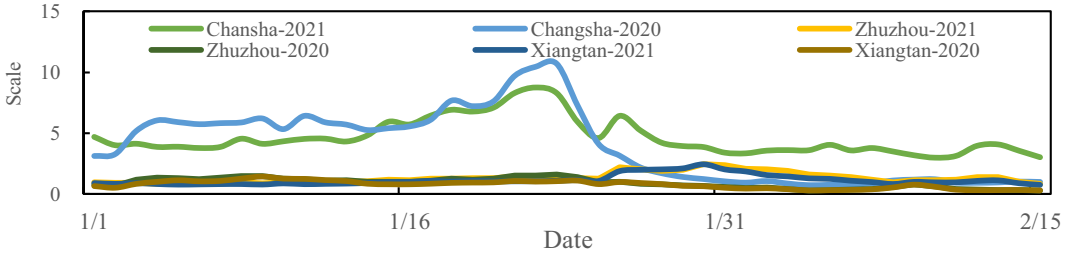

(d). the total move-out scale of Changsha, Zhuzhou and Xiangtan

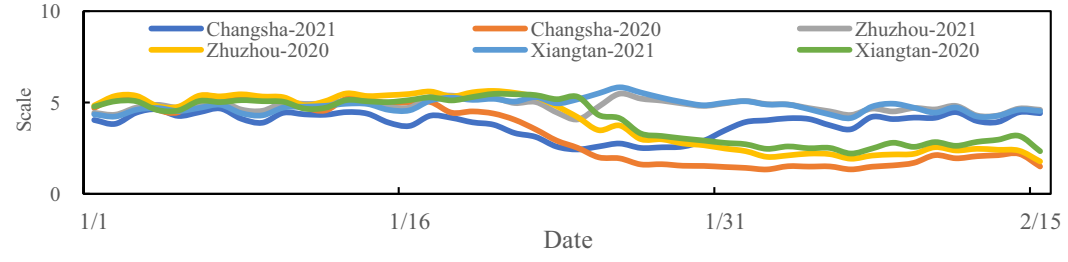

(e). the amount of travel and migration inside city of Changsha, Zhuzhou and Xiangtan

Fig. 7. Baidu migration data for each city of Chang-Zhu-Tan.
(a). Percentage of Changsha migrating to Zhuzhou and Xiangtan.
(b). Percentage of Zhuzhou migrating to Changsha and Xiangtan.
(c). Percentage of Xiangtan migrating to Changsha and Zhuzhou.
(d). the total move-out scale of Changsha, Zhuzhou and Xiangtan.
(e). the amount of travel and migration inside city of Changsha, Zhuzhou and Xiangtan.

5.1. Weights of population migration

There has been a significant correlation between population flow and the development of COVID-19 (Brockmann & Helbing, 2013), which makes the analysis of population flow quite helpful for this epidemic's simulation. According to the related intercity migration scale calculated using Eq. (1), we applied the chord diagram to analyze the population flow weights of four cities, namely the three in the Chang-Zhu-Tan agglomeration and Wuhan. The chord diagram is a digital visualization method used to disclose the relationships between data in a matrix. It is mainly composed of nodes and chords. The node data are arranged radially along the circumference, while the weighted (with width) arc connecting any two points on the circle is called a chord, and the chord (the connecting arc between the two points) represents the correlation between the two points. Furthermore, the quantity of nodes in the chord diagram refers to the current target number, and the contact area between the arc and the node (the thickness of the chord) demonstrates the degree of relationship or proportional relationship between two target data points.

Fig. 8 shows the changes in the population flow weights from before to after the outbreak, and it can be observed that there is no significant change in the pattern of population flow in the Chang-Zhu-Tan urban agglomeration, but that the weight of the population flow imported from other cities to Chang-Zhu-Tan decreases after the outbreak. It is interesting to note that after 23 January, there was still population mobility within and between other cities in the urban agglomeration. Possible reasons for this are the following five special cases where travel within and between urban agglomerations is still possible. 1. military vehicles, police vehicles, ambulance, fire-fighting, rescue, sanitation and cleaning and other special vehicles; 2. vehicles undertaking tasks such as specimen delivery, medical emergencies, epidemic prevention materials and personnel transportation, command and dispatch and other epidemic prevention and control tasks; 3. vehicles transporting pregnant women awaiting delivery, seriously ill people seeking medical treatment and other emergency situations; 4. vehicles for the protection of the livelihood of the public;5. other vehicles with unit certificates for work purposes. Therefore, there is still population movement after a public health event. Each province declared a first-level response to major public health emergency after January 23, 2020. It is unlikely that other cities across the country will have exported cases to the Chang-Zhu-Tan urban agglomeration after this policy was enacted. Based on this control situation and the incubation period of the virus itself, the total number of cases imported into the urban agglomeration from other cities may have a strong correlation with the scale of the population migration in the first five days (Xing et al., 2020). Therefore, the predicted scale of the population migration into this urban agglomeration from other cities was taken from the five days prior to the emergence of infected cases in the Chang-Zhu-Tan urban agglomeration. For example, cases diagnosed in this urban agglomeration on January 24, 2020 were correlated with the population that migrated from other cities on January 19, 2020 (Fig. 9).

5.2. Model analysis

The time delay between the onset of symptoms of COVID-19 and case reporting is noteworthy (S. J. Lai, Ruktanonchai, Zhou, Prosper, et al., 2020b; Xu et al., 2020). As a result of this delay, the number of reported confirmed cases cannot be used directly to evaluate the accuracy of our model. According to the "China-WHO Novel Coronavirus Pneumonia (COVID-19) Joint Investigation Report", it was found that the process of confirming COVID-19 cases is very complicated. When suspected symptoms are discovered, the suspected patient's data should be reported to the municipal level, which should review the report, and if it was found to be positive then report it in turn to the provincial level. A case will be classified as a confirmed case of COVID-19 after it has been rechecked and found to be positive by the provincial experts. After the diagnosis is confirmed, the local disease prevention and control center will then need to report the confirmed case information to the provincial CDC, and then to the provincial health commission, which will then release the province's aggregated data the next day at 3 p.m. It takes two days from the onset of symptoms of COVID-19 to confirm the diagnosis with the case reporting process (China, 2020). Thus, the time delay between the onset of symptoms and the case reporting of COVID-19 is two days. This is largely consistent with the findings of the study by Lai et al. (S. J. Lai, Ruktanonchai, Zhou, Prosper, et al., 2020b). We consider this a two-day time delay and recount the number of confirmed cases on that day. For example, if the number of confirmed cases in city X is reported to be 1000 on February 10, then it is assumed that the number of

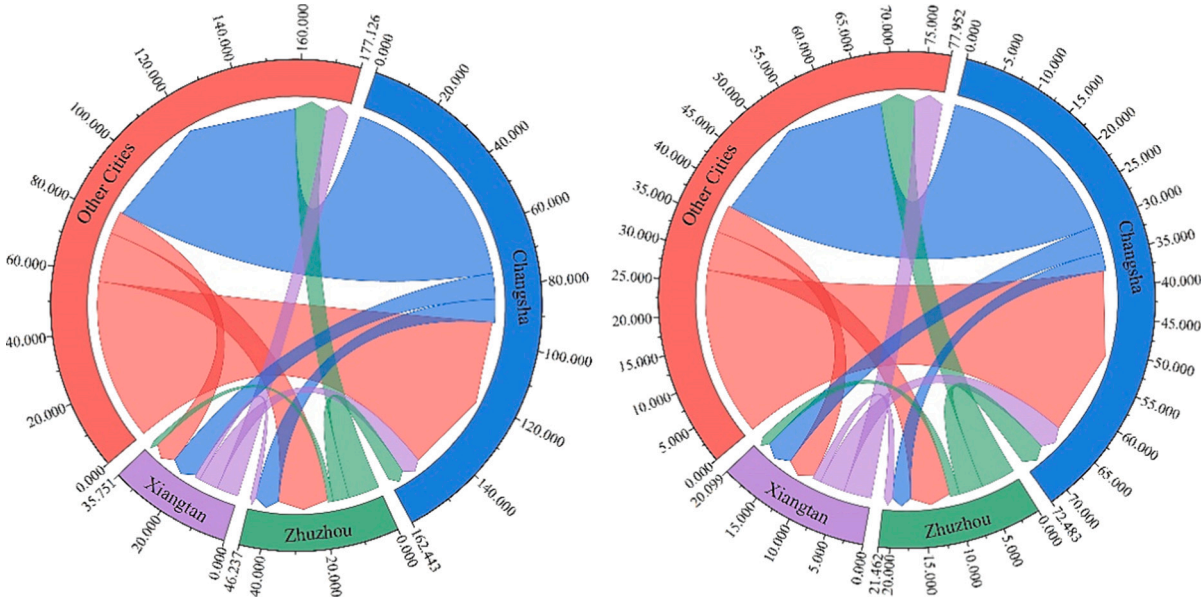

Fig. 8. Weight map of population flow between Chang-Zhu-Tan urban agglomeration and other cities.

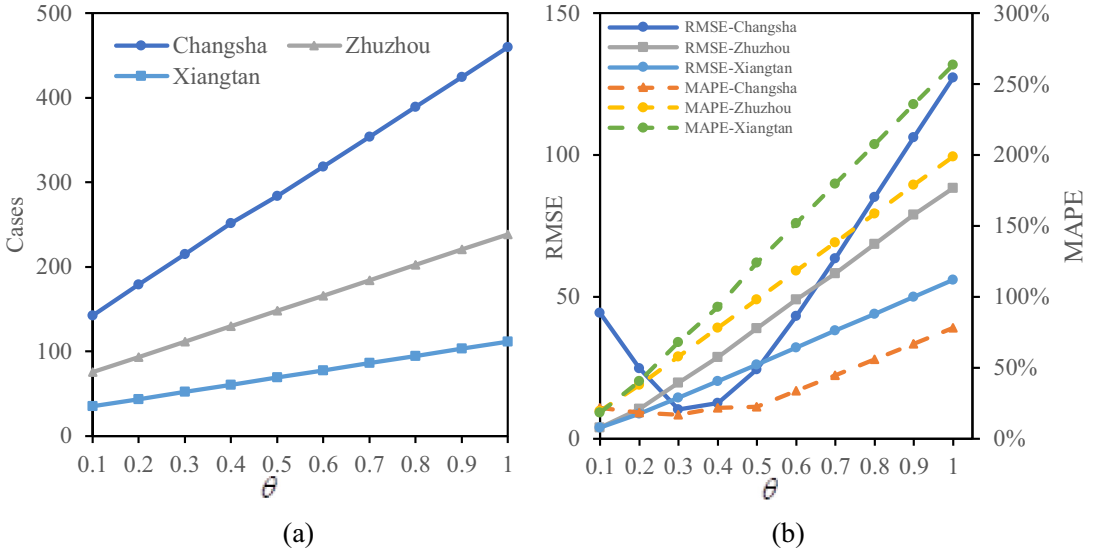

Fig. 9. (a) Cases under different θ; (b) RMSE and MAPE.

infectious disease cases in city X on February 8 is also 1000.

5.2.1. Robustness

In this subsection, we test the robustness of the model by adjusting the sample in the following ways: (a) A robustness test for a smaller-scale epidemic. An epidemic rebound event from July 28, 2021 to August 15, 2021, with Zhangjiajie as the center of the epidemic, is selected. The outbreak also involved Changsha, Xiangtan, and Zhuzhou, with 71, 2, 2, and 21 confirmed cases in the four cities, respectively, representing smaller-scale outbreak rebound events. We performed linear regression analysis and error analysis on the real and estimated cases, and the results are shown in Table 3. (b) Simulation of the epidemic for the non-Chinese New Year period when an outbreak of a certain scale occurred. To explore the robustness of the model in other time periods, a recent epidemic rebound in Sanya, which was the center of the epidemic, was selected. The outbreak affected 10 prefectural cities and states in Hainan Province, with a cumulative number of confirmed cases of 8530, representing a large-scale outbreak rebound event during the non- Chinese New Year, from August 1 to September 3, 2022. Again, the results of the regression analysis are shown in Table 4.

The analysis of the results in Tables 3 and 4 shows that the precision and accuracy of our established UAEMM is low for outbreaks that do a smaller-scale epidemic, but for simulations of outbreaks of a certain scale, it does perform well and is robust at any stage.

5.2.2. Sensitivity

We also perform a sensitivity test for the empirical parameter θ in eq. (3). We fix the values of the other factors, set the initial value of θ to 0.1, and observe the case development of each city as θ increases to 1 with an increment of 0.1. We also compare RMSE and MAPE as θ increases.

The sensitivity analysis of θ shows that the move-out of the model (number of cases) is sensitive to θ and positively correlated with it. By comparing the slopes for the cities, the number of cases is more sensitive to θ in Changsha than in Zhuzhou and Xiangtan, and the number of cases in Xiangtan has the lowest sensitivity. From the perspective of error, for the Changsha cases, MAPE changes little as θ increases from 0.1 to 0.5, and then increases gradually as θ increases from 0.5 to 1, while RMSE decreases and then increases as θ increases from 0.1 to 1. In Zhuzhou and Xiangtan, both RMSE and MAPE increase with the increase in θ.

Table 3
Simulation of indicators related to the Zhangjiajie outbreak.

City	R^2	RMSE	MAPE
Zhangjiajie	0.897	6.955	23.061 %
Changsha	0.338	2.225	97.328 %
Zhuzhou	0.878	7.780	28.382 %
Xiangtan	0.614	2.281	94.966 %

Note: RMSE is root mean square error; MAPE is mean absolute percentage error; R^2 is the goodness-of-fit.

Table 4
Simulation of indicators related to the Sanya outbreak.

City	R^2	RMSE	MAPE
Sanya	0.993	7.477	2.188 %
Ledong	0.986	2.651	9.629 %
Zhanzhou	0.934	2.170	3.600 %
Dongfang	0.973	3.104	3.027 %
Wanning	0.948	3.819	6.235 %
Lingshui	0.917	2.923	5.784 %
Lingao	0.906	8.520	9.633 %
Haikou	0.906	9.862	8.257 %
Chengmai	0.881	8.332	7.152 %

5.2.3. Policy factor and distance decay factor

Based on the timing of the traffic control measures enacted for each city, that is the policy intervention nodes, we solve for the policy effects of the three traffic control measures, namely, the public health event level 1 response, traffic blockade in epidemic-affected areas and public transportation shutdown in each city, using the big data from Baidu migration from the same period of the 2021 lunar calendar as the control group, and present the results in the following Table 5.

We obtain the distance decay factors of the different cities and the Chang-Zhu-Tan urban agglomeration. The constant d_0 takes the straight-line distance between Shuangyu and Kashgar, which is 5414 km. The distance attenuation factor among the members of the Chang-Zhu-Tan urban agglomeration takes values between 0.915 and 0.912, and the distance attenuation factor between the other cities and Chang-Zhu-Tan is between 0.016 and 0.889.

5.2.4. Accuracy analysis

To assess the accuracy of the model, we apply the UAEMM and CEMM to simulate the number of COVID-19 cases in each city of the Chang-Zhu-Tan urban agglomeration from January 24, 2020 to February 15, 2020. Fig. 10 shows the results of the linear regression

Table 5
Effects of different measures in Chang-Zhu-Tan.

City	Level 1 response			Traffic blockades in infected areas			Public transportation shutdown		
	IIM	IM	IIN	IIM	IM	IIN	IIM	IM	IIN
Changsha	−0.317***	−0.164***	−0.403***	−0.437***	−0.415***	−0.307***	−0.569***	−0.592***	−0.448***
Zhuzhou	−0.467***	−0.329***	−0.480***	−0.484***	−0.507***	−0.374***	−0.657***	−0.615*	−0.394*
Xiangtan	−0.517***	−0.301***	−0.422***	−0.411***	−0.480***	−0.435***	−0.565***	−0.498	−0.322

Note:1. IIM indicates the impact of the traffic control measures on inward migration scale; IM indicates the impact of the traffic control measures on outward migration scale; IIN indicates the impact of the traffic control measures on inner-city activities. 2.*, **, *** denote $p < 0.1$, $p < 0.05$, $p < 0.01$.

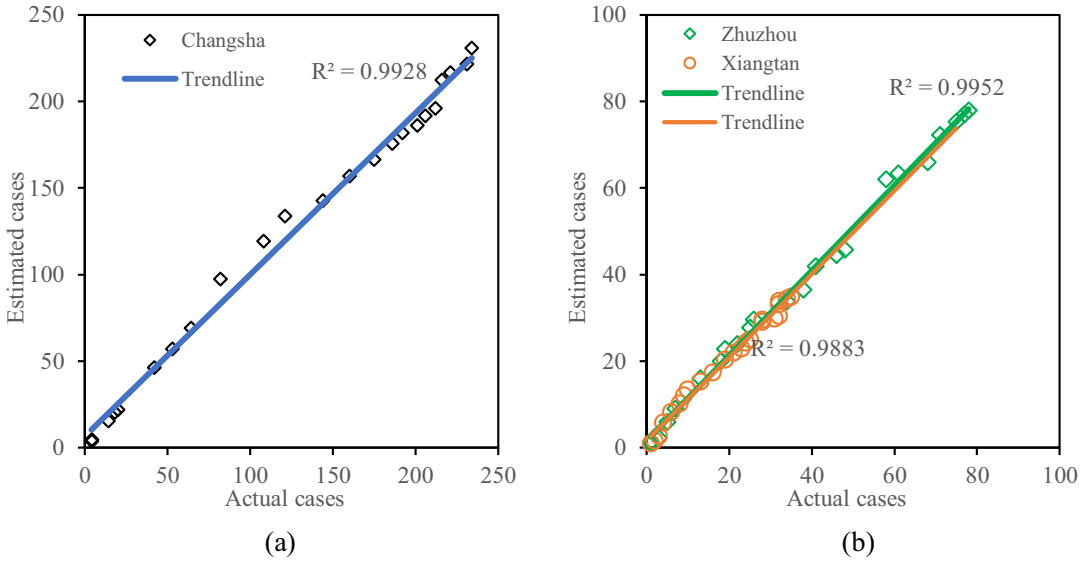

Fig. 10. Scatter plot of actual and estimated cases in Chang-Zhu-Tan urban agglomeration.

analysis between the estimated cases and the actual cases of the officially published number of infection cases in each city. Table 6 presents the assessment of errors, using indicators such as RMSE (Root-Mean-Square-Error) and MAPE (Mean-Absolute-Percentage-Error). Overall, the model still has some accuracy in simulating the spread and spatial diffusion of the epidemic.

Table 6
Accuracy analysis of UAEMM and CEMM for the Chang-Zhu-Tan urban agglomeration.

Model	City	R^2	MAPE	RMSE	Std. error	sig
UAEMM (without considering distance attenuation)	Changsha	0.949	22.125 %	12.339	0.048	0.000
	Zhuzhou	0.989	27.153 %	7.800	0.025	0.000
	Xiangtan	0.991	26.581 %	9.540	0.017	0.000
UAEMM (considering distance attenuation)	Changsha	0.990	16.716 %	9.850	0.033	0.000
	Zhuzhou	0.992	19.168 %	3.362	0.024	0.000
	Xiangtan	0.935	18.461 %	5.172	0.016	0.000
UAEMM (Considering distance decay and decreasing returns to scale)	Changsha	0.993	7.740 %	8.617	0.017	0.000
	Zhuzhou	0.995	10.258 %	2.052	0.015	0.000
	Xiangtan	0.988	11.970 %	1.545	0.023	0.000
CEMM	Changsha	0.820	39.078 %	20.158	0.076	0.000
	Zhuzhou	0.886	50.797 %	10.736	0.085	0.000
	Xiangtan	0.846	68.804 %	18.772	0.104	0.000

5.3. Composition of cases in urban agglomeration

Based on the UAEMM, we roughly estimate the composition of cases of disease imported from the cities outside of the urban agglomeration, and the urban agglomeration members. From January 24, 2020 to February 4, 2020, the percentage of cases imported from non-members of the urban agglomeration into the urban agglomeration was 36.40 %, and the percentage of cases coming from urban agglomeration members was 63.60 % (as shown in Fig. 11(a)). Therefore, urban agglomerations should focus on preventing intra-urban-agglomeration transmission, which may be due to the spatial structure of urban agglomerations, featuring not only highly developed transportation links between members but also many economic ties, making the internal prevention and control of disease among urban agglomeration members a greater issue.

Specifically, the cases in the core city of Changsha, a member of the urban agglomeration, are made up of 54.5 % internal cases and 45.50 % imported cases, with 37.3 % of the cases imported from external cities, and 4.7 % and 3.4 % imported from Zhuzhou and Xiangtan, members of the urban agglomeration, respectively (as shown in Fig. 11(b)). This implies that, when an epidemic occurs in Changsha, the population flow within the city should be controlled, firstly to prevent the spread of cases within the city, and secondly to prevent the influx of cases from cities that do not belong to the urban agglomeration, such as Wuhan, which was the center of the epidemic, and is immediately adjacent to Changsha, and Guangzhou and Shenzhen from where an influx of population into the Chang-Zhu-Tan urban agglomeration occurs in Chinese New Year. Zhuzhou city's cases comprise 26.9 % internal cases and 73.1 %

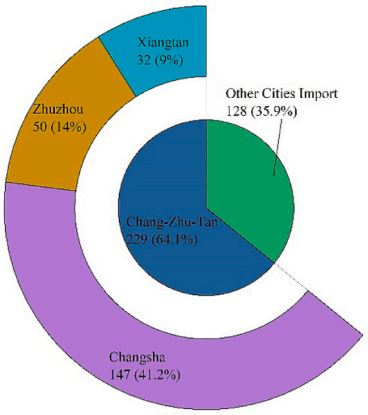

(a) COVID-19 case composition of Chang-Zhu-Tan

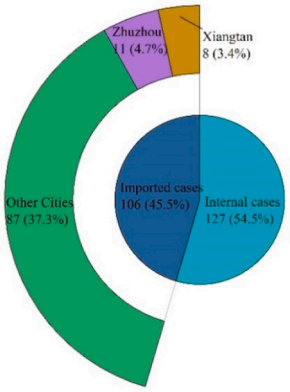

(b) COVID-19 case composition of Changsha

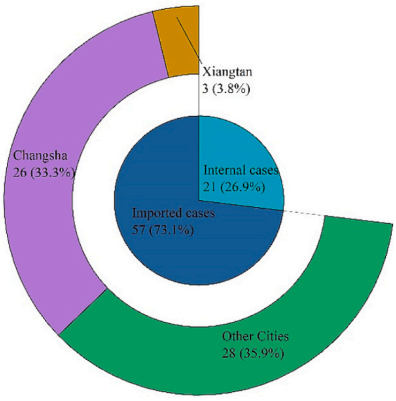

(c) COVID-19 case composition of Zhuzhou

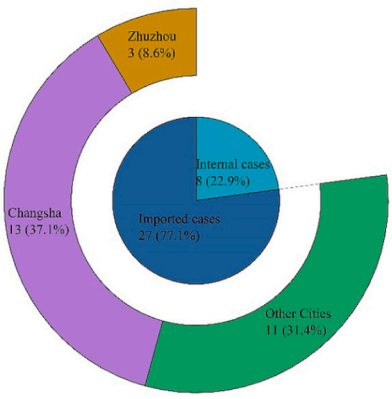

(d) COVID-19 case composition of Xiangtan

Fig. 11. Composition of cases.
(a) COVID-19 case composition of Chang-Zhu-Tan.
(b) COVID-19 case composition of Changsha.
(c) COVID-19 case composition of Zhuzhou.
(d) COVID-19 case composition of Xiangtan.

imported, with 33.30 % of cases imported from Changsha city and 35.9 % of cases imported from other cities outside of the urban agglomeration (as shown in Fig. 11(c)). The composition of cases in Xiangtan and Zhuzhou was similar, but Xiangtan has a higher percentage of imported cases from Changsha (as shown in Fig. 11(d)). Thus, when an epidemic occurs in Zhuzhou and Xiangtan, their connections – both transportation and economic – with Changsha, the central city of the urban agglomeration, should be cut off first, and then measures such as checking the nucleic acid certificate, landing quarantines or banning entry should be implemented for other cities, according to the actual epidemic situation in those cities, to prevent the importation of cases. As for the intracity population movement, unlike in Changsha, a travel ban strategy does not have to be implemented, and economic intracity activities can be allowed under certain prevention and control measures.

5.4. *Effect of traffic control measures in urban agglomerations*

The theoretical values of infection case were calculated using the Baidu migration data for the same period of the 2021 lunar calendar, for a natural development state (without considering any medical or non-medical interventions, etc.), in the Chang-Zhu-Tan urban agglomeration. In order to study the development of the epidemic under different traffic control measures, three traffic control measures were simulated, namely the first-level response to major public health emergency (labeled P1), traffic blockades in infected areas (P2) and public transportation shutdown (P3). The effectiveness of these traffic control measures will now be analyzed from three perspectives.

1. The impact of the traffic control measures on cases in the Chang-Zhu-Tan urban agglomeration

If the Chang-Zhu-Tan urban agglomeration had not taken any means of epidemic prevention or control and allowed the epidemic to develop freely, the total number of cases would theoretically have been 11.61 times the number of actual cases, by February 15, 2020, of which the number of cases imported from non-members of the urban agglomeration would have been 3165 cases, 25.12 times the actual number of cases, while the number coming from all members of the Chang-Zhu-Tan urban agglomeration would have been 3.14 times the actual number of cases. The epidemic prevention and control measures taken by the Chang-Zhu-Tan urban agglomeration effectively controlled the development of the epidemic. Comparing the development of the epidemic in the Chang-Zhu-Tan urban agglomeration under the different measures, we found that the first-level response to major public health emergency had the best effect in interrupting the spread of cases, which might be related to the time those measures were promulgated, the level of the decision making, and the organization and implementation of the emergency response. We also calculated the percentage difference between theoretical cases and actual cases under the different traffic control measures. The three traffic control measures reduced the number of imported cases by between 84.87 % and 92.74 %, while cases coming from within the urban agglomeration were reduced by between 38.71 % and 58.06 %, showing that the traffic control measures were more effective in preventing and controlling the number of cases imported into the urban agglomeration. The development of the epidemic under the different measures is shown in Fig. 12(a), and the composition of cases in the Chang-Zhu-Tan urban agglomeration under the different measures is shown in Fig. 12(b).

2. Impact of traffic control measures on the cases in each member city of the Chang-Zhu-Tan urban agglomeration

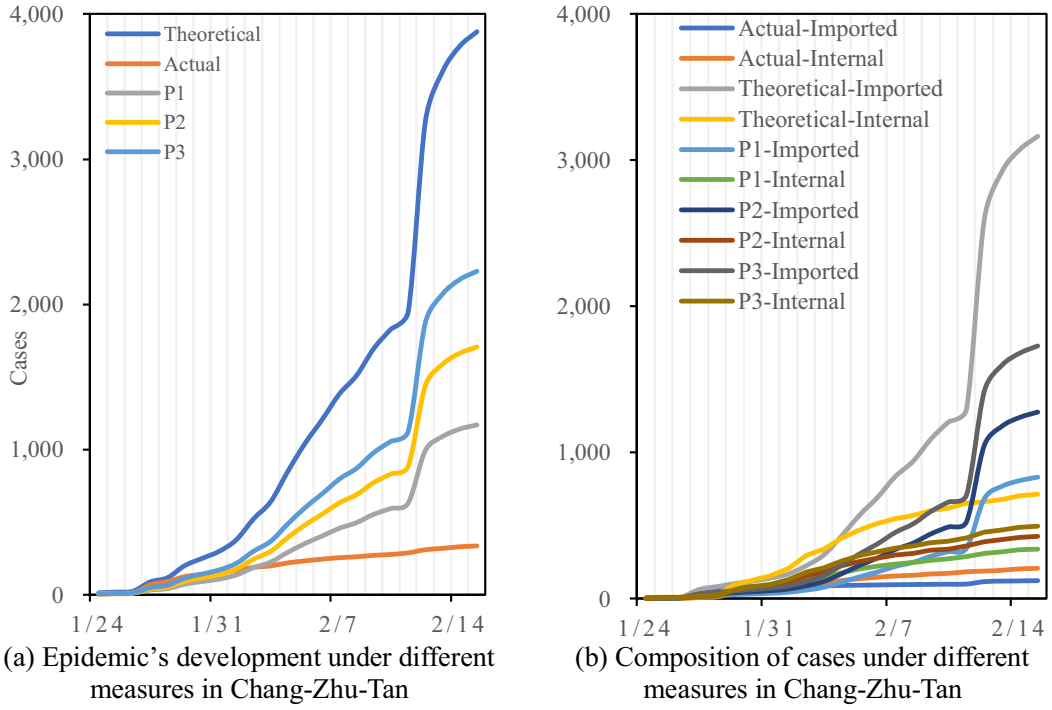

Fig. 12. Total number and types of cases in Chang-Zhu-Tan under different measures.
(a) Epidemic's development under different measures in Chang-Zhu-Tan.
(b) Composition of cases under different measures in Chang-Zhu-Tan.

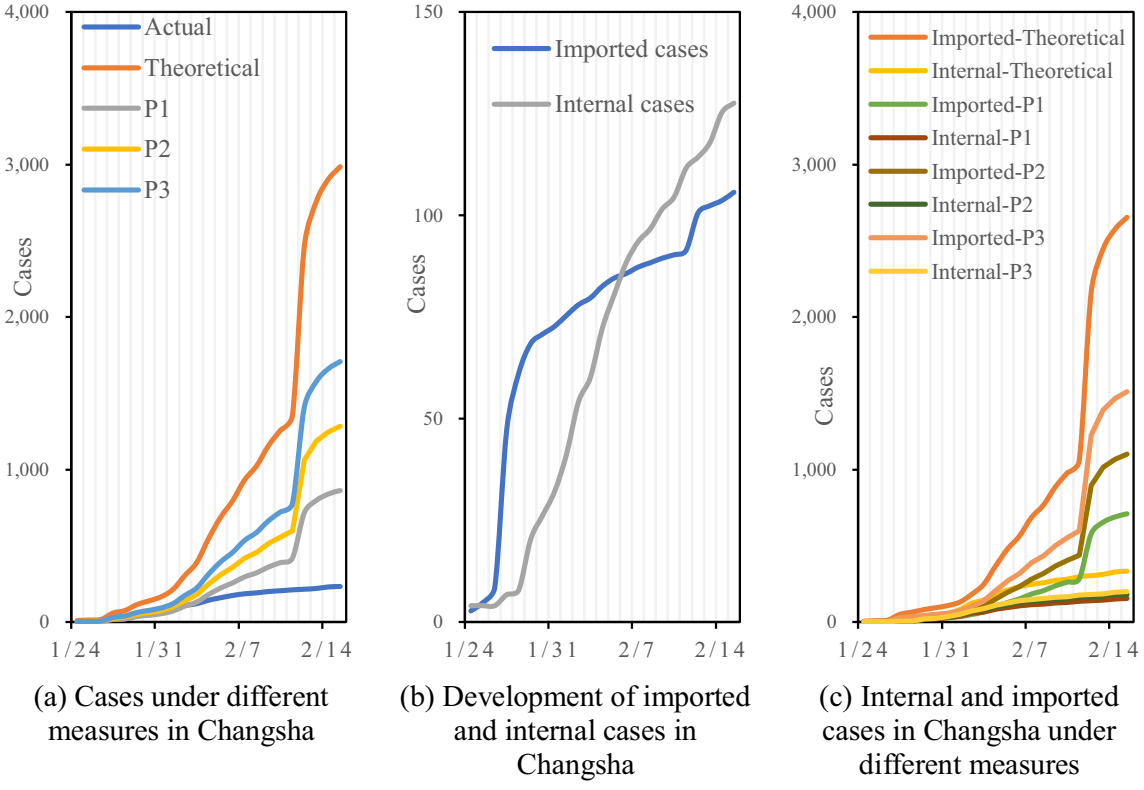

Fig. 13. Epidemic situation in Changsha.
(a) Cases under different measures in Changsha.
(b) Development of imported and internal cases in Changsha.
(c) Internal and imported cases in Changsha under different measures.

Comparing the total number of cases in each city, the first-level response to major public health emergency is still the most effective in interrupting the spread of cases, followed by traffic blockades in infected areas, with the public transportation shutdown least effective (Figs. 13(a), 14(a) and 15(a)). However, it is worth noting that, in the early stages of the epidemic, Changsha city was dominated by imported cases while, after February 6, the number of internal cases dominated the number of imported cases, implying that Changsha city needed to adjust the focus of its epidemic prevention and control after February 6 (Fig. 13(b)). Comparing the effectiveness of the different measures in blocking internal and external cases in the city, it is clear that the three measures of the first-level response to major public health emergency, traffic blockades in infected areas and a public transportation shutdown were more effective in blocking imported cases, while the control of internal cases in the city was highly uniform and did not differ significantly across the measures (Figs. 13(b)(c), 14(b)(c) and 15(b)(c)). This is also consistent with our analysis of the composition of urban cases in Section 5.3, where Zhuzhou and Xiangtan faced a greater risk of external than internal urban transmission, indicating that the measures developed by the policy makers were effective and precise. Also, comparing the prevention and control effects of each measure in different cities, we found that the first-level response to major public health emergency was more effective in preventing and controlling the outbreak in Changsha, while the public transportation shutdown measure achieved the best prevention and control effect in Xiangtan, and the traffic blockades in infected areas achieved good results in blocking the internal transmission in each city.

3. Effect of traffic control measures on the mutual propagation among members of the urban agglomeration

Fig. 16(a)-(c) show the real inter-transmission among cities, while Fig. 16(d)-(f) show that under different measures. In terms of the cases imported into Changsha, the number imported from Zhuzhou is greater than that from Xiangtan. Therefore, the traffic control measures enacted in Changsha were more effective at blocking the importation of cases from Zhuzhou, and the effects of the three traffic control measures range from 44.42 % to 73.33 %, showing again that the first-level response to major public health emergency was the best measure. Interestingly, the traffic control policy in Changsha was less effective in blocking imported cases from Xiangtan than from Zhuzhou, but no cases were imported into Changsha after February 8, probably due to the small scale of the outbreak in Xiangtan itself and the absence of any concentrated outbreak around February 8. Therefore, after February 8, Changsha could adjust its measures appropriately and resume some economic activities with lower risk under certain conditions. Changsha was the largest source of input cases for Zhuzhou, and the traffic control policy adopted by Zhuzhou reduced the influx from Changsha by >67.59 %, while it was not effect at reducing the number of cases imported from Xiangtan. Xiangtan has a similar case composition to Zhuzhou, with a reduction of >51.09 % of the cases imported from Changsha following the implementation of the measures. This also gives us the insight that cities with similar case compositions could learn from each other's experience in prevention and control.

6. Discussion and conclusion

6.1. Discussion

Compared with some past studies, the UAEMM developed in this study is more applicable to the study of intercity epidemic transmission. First, the model is based on the reality of intercity transportation networks and the theory of correlation between intercity population mobility and infectious diseases, whereas traditional infectious disease models only consider transmission within a single city or case output from an epidemic center. Examples include the SIR-M proposed by

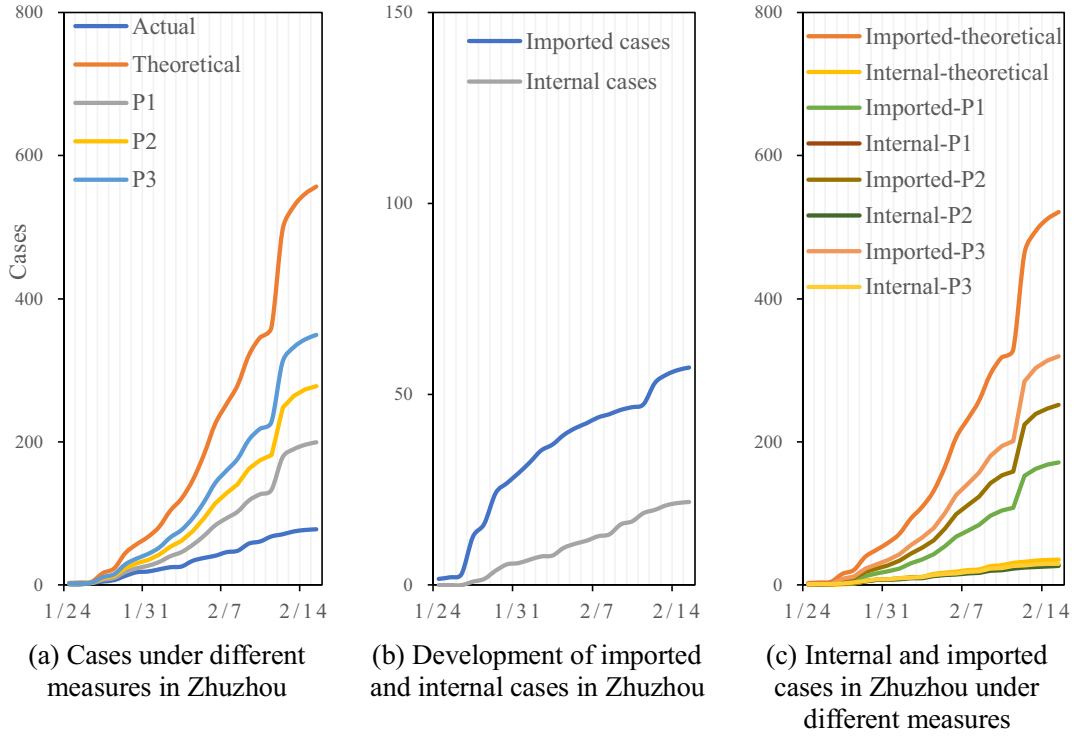

Fig. 14. Epidemic situation in Zhuzou.
(a) Cases under different measures in Zhuzhou.
(b) Development of imported and internal cases in Zhuzhou.
(c) Internal and imported cases in Zhuzhou under different measures.

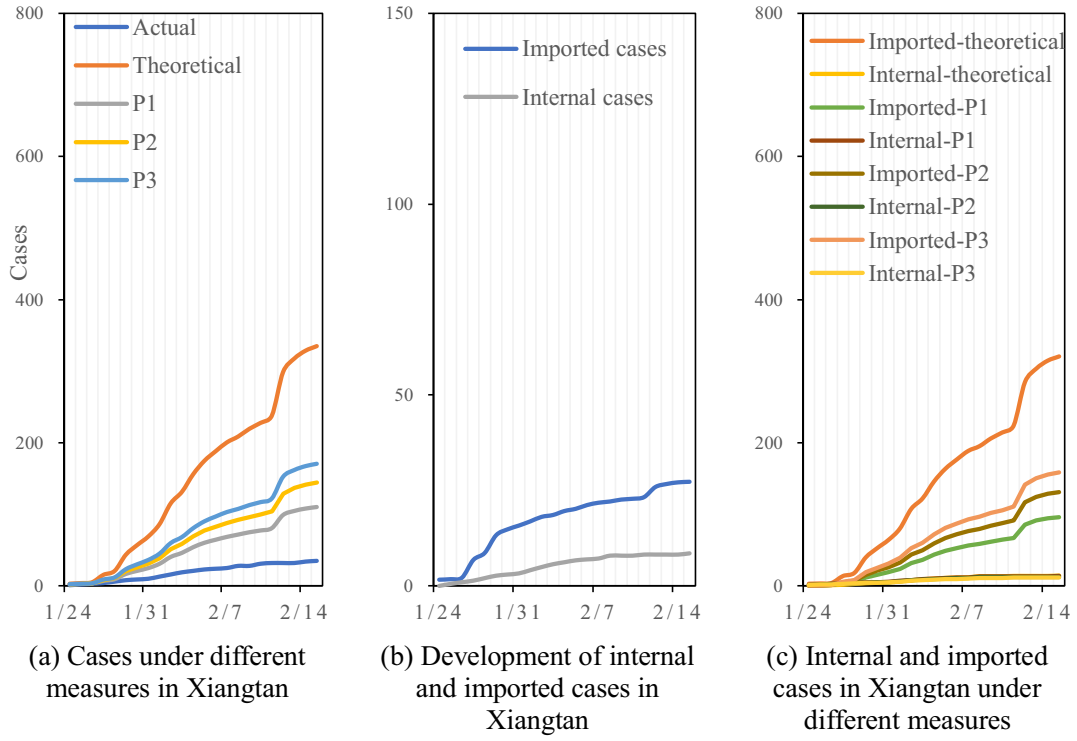

Fig. 15. Epidemic situation in Xiangtan.
(a) Cases under different measures in Xiangtan.
(b) Development of internal and imported cases in Xiangtan.
(c) Internal and imported cases in Xiangtan under different measures.

Muley et al. (Muley et al., 2021) traditional room models such as the SEIR developed by Liu et al. (Jielun Liu et al., 2022) and the deep-learning models proposed by Chimmula and Zhang (Chimmula & Zhang, 2020). These studies were mostly set in a closed space and only looked at the evolutionary pattern of the epidemic within the city, making it difficult to obtain information on intercity transmission. In contrast, we view each city in our study population as an outbreak center exporting cases to other cities (Fig. 2), which gives our model an intercity perspective and allows us to estimate the risk of cases imported from different cities, better reflecting the characteristics of case transmission from an intercity perspective. Second, compared with Wei et al.'s (Wei et al., 2021) study, our model compensates for the inability of the CEMM to simulate specific urban structures, by considering urban inputs and active intra-urban populations, sharpening the focus on internal and external prevention and control. Finally, our model can accurately identify the sources of cases for the members of an urban agglomeration, and evaluate the effectiveness of various traffic control measures, which was not mentioned by Liu (J. Liu et al., 2021) in his discussion on the prevention and control of urban epidemics.

Based on the results of this paper, we will now make some extended proposals, which are practical points that are applicable not only to the Chang-Zhu-Tan urban agglomeration but to epidemic control in other urban agglomerations as well.

The first concerns epidemic prevention and control in urban agglomerations. In the early stages of an epidemic, urban agglomerations face the likelihood of cases being imported from cities outside the urban agglomeration, including cities at the center of the epidemic and other cities that have reached a certain level of epidemic and population interaction. Simultaneous adoption of the first-level response to major public health emergency by urban agglomeration members was the most effective means of interrupting the importation of cases from outside cities into the urban agglomeration. Traffic closures in infected areas were more effective than public transportation shutdowns. This may be related to the timing of the measures, the level of decision making, and the organization and implementation of the emergency response. The first-level response to major public health emergency is a unified preventive and control measure taken at the provincial level in Hunan Province, which has a high degree of uniformity, and a compulsory impact on all members of the urban agglomeration, and will attract the attention of all administrative departments in each city, thus potentially reaping better preventive and control effects. This is consistent with the findings of Mayer's (Mayer & Boston, 2022) study of an “alert-level system” similar to this policy in New Zealand. However, it contrasts with the findings from Liu's (S. Liu & Yamamoto, 2022) study of “a state of emergency” in Japan, which was not mandatory and therefore did not achieve as good results in containing the epidemic in Japan.

In addition, we found that the case structure of the core cities in the urban agglomeration changed as the epidemic developed, based on the results of the case study, e.g., the number of imported cases in Changsha, the core city in the Chang-Zhu-Tan urban agglomeration, was greater than the number of intracity-transmitted cases from January 24, 2020 to February 6, 2020, while after February 6, the case structure in Changsha changed, with more internal than imported cases (Fig. 14 (b)). However, this was not the case in the other, auxiliary cities, where the imported cases were always more than the internally transmitted ones (Figs. 15 (b), 16(b)). A possible reason for this could be the gradual resumption of intracity traffic, as well as economic activities in Changsha, starting on February 6. The implication of this is that, as a core city in the urban agglomeration, it is important to gradually adjust the epidemic prevention and control policy regarding social activities, with the prevention of imported cases being the main focus in the early stages of the epidemic, while the management of the active population in the city should be a priority when economic activities within the city resume. There is no need for home isolation, travel restrictions and other more stringent measures, but it is necessary to require residents to wear a good mask and maintain social distance (Aghabayk et al., 2021).For auxiliary

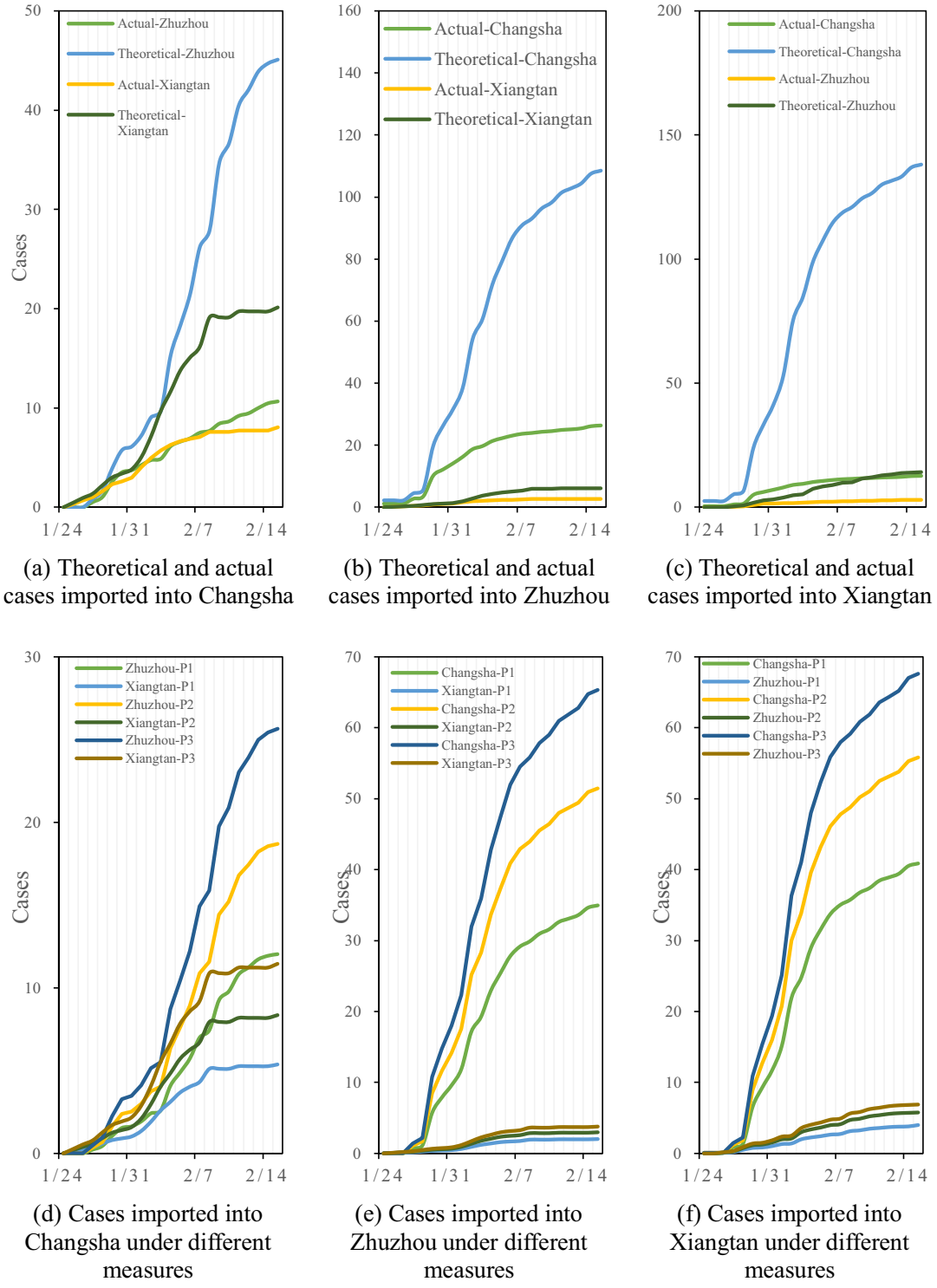

Fig. 16. Mutual propagation of cases between the members of Chang-Zhu-Tan under different measures.
(a) Theoretical and actual cases imported into Changsha.
(b) Theoretical and actual cases imported into Zhuzhou.
(c) Theoretical and actual cases imported into Xiangtan.
(d) Cases imported into Changsha under different measures.
(e) Cases imported into Zhuzhou under different measures.
(f) Cases imported into Xiangtan under different measures.

cities, preventing the importation of cases should remain the focus of outbreak prevention and control.

The spatial pattern of "one main and two auxiliary" or "one main and many auxiliary" in the Chang-Zhu-Tan urban agglomeration is common all over the world, for example in the Pearl River Delta urban agglomeration in China. Examples from other countries include the Chicago-Pittsburgh urban agglomeration in the U.S., the London urban agglomeration in the United Kingdom and the Greater Paris urban

agglomeration in France. These urban agglomerations are economically prosperous, with close population interaction and highly developed transportation network patterns among their members. They are also currently suffering from the COVID-19 epidemic, and the UAEMM and related parameter calculations proposed in this paper are equally applicable to other urban agglomerations, requiring only local epidemiological statistics and population migration data. Furthermore, the research framework and the findings in this paper may have the potential to be applied to other countries for similar research purposes, which gives the study an international perspective and global relevance.

This study can be used as a starting point for studying epidemic prevention and control in urban agglomerations. It should also be noted that it has some limitations: firstly, the UAEMM proposed in this paper is only applicable to the simulation of epidemics of a certain scale, and has low accuracy for smaller-scale epidemics; secondly, many traffic control measures are implemented simultaneously, and their impacts superimposed, while our treatment is too simple when we study individual measures; finally, we only consider propagation between cities within a country, while transmission between countries should also be considered.

6.2. Conclusion

With the development of global urbanization, urban agglomerations and metropolitan areas will become more and more common, and dealing with the prevention and control of infectious diseases will become a more complex issue in the future. In this paper, we have proposed a UAEMM with an urban perspective for studying the spread of epidemics in urban agglomerations. The model can be used to analyze case composition in cities and urban agglomerations, to simulate intercity propagation and to evaluate the effectiveness of traffic control measures taken. The Chang-Zhu-Tan urban agglomeration was selected for validation purposes. The main findings are as follows: (1) The proposed UAEMM shows some accuracy in simulating the spread of cases between cities and is applicable for all time periods, but has low accuracy for smaller-scale outbreaks. (2) The pressure on prevention and control faced by urban agglomerations mainly comes from the spread among members of the agglomeration; the composition of the cases in core cities is likely to change with policy changes, requiring a dynamic adjustment of prevention and control measures, and auxiliary cities should always do their best to prevent imported cases. (3) The first-level response to major public health emergency, transportation blockades in infected areas and public transportation shutdown measures have obvious effects in interrupting the spread of cases. The three measures complement each other, and their combined use improves epidemic prevention and control. In terms of individual measures, the first-level response to major public health emergency works best.

In addition, there are some ideas for future studies that need to be mentioned. The pattern and probability of case transmission in urban agglomerations under different shares of commuting modes could be studied. In addition, since the strain of COVID-19 is constantly mutating, infectious disease models can be developed to cope with different strain characteristics. Finally, considering the large number of urban agglomerations in China and the recent changes in policy for epidemic control, our further work is to explore the pattern of case transmission between other urban agglomerations, to identify the composition of cases in different urban agglomerations, to evaluate the effectiveness of current epidemic control policies, and to demonstrate the wider suitability of the proposed method.

Declaration of competing interest

The authors declare that they have no known competing financial interests or personal relationships that could have appeared to influence the work reported in this paper.

Data availability

The authors do not have permission to share data.

Acknowledgments

The research described here was supported by the Chinese Fundamental Research Funds for the Central Universities (2021RC280), the National Natural Science Foundation of China (71931003, 52102405), the Natural Science Foundation of Hunan Province (2021JJ40603) and the Scientific Research Program of the Education Department of Hunan Province (21B0335, 20B009).

CRediT authorship contribution statement

Wang Xiang: Conceptualization, Methodology, Writing- Original draft preparation.; **Li Chen:** Methodology, Software, Writing-Original draft preparation, Writing-Reviewing and Editing.; **Xuedong Yan:** Supervision, Funding acquisition.; **Bin Wang:** Data curation, Investigation.; **Xiaobing Liu:** Supervision, Writing-Reviewing and Editing, Project administration.

References

Aghabayk, K., Esmailpour, J., & Shiwakoti, N. (2021). Effects of COVID-19 on rail passengers' crowding perceptions. *Transportation Research Part A: Policy and Practice, 154*, 186–202. https://doi.org/10.1016/j.tra.2021.10.011

Arino, J., Jordan, R., & van den Driessche, P. (2007). Quarantine in a multi-species epidemic model with spatial dynamics. *Mathematical Biosciences, 206*(1), 46–60. https://doi.org/10.1016/j.mbs.2005.09.002

Beck, M. J., Hensher, D. A., & Nelson, J. D. (2021). Public transport trends in Australia during the COVID-19 pandemic: An investigation of the influence of bio-security concerns on trip behaviour. *Journal of Transport Geography, 96*, Article 103167. https://doi.org/10.1016/j.jtrangeo.2021.103167

Brockmann, D., & Helbing, D. (2013). The hidden geometry of complex, network-driven contagion phenomena. *Science, 342*(6164), 1337–1342. https://doi.org/10.1126/science.1245200

Cantuarias-Villessuzanne, C., Weigel, R., & Blain, J. (2021). Clustering of European smart cities to understand the cities' sustainability strategies. *Sustainability, 13*(2). https://doi.org/10.3390/su13020513

Chen, H., Shi, L., Zhang, Y., Wang, X., & Sun, G. (2021). Guangdong's experience in defeating the COVID-19. *Medicine, 100*(18). https://doi.org/10.1097/MD.0000000000025881

Chen, X., Zhang, A. Y., Wang, H., Gallaher, A., & Zhu, X. L. (2021). Compliance and containment in social distancing: Mathematical modeling of COVID-19 across townships. *International Journal of Geographical Information Science, 35*(3), 446–465. https://doi.org/10.1080/13658816.2021.1873999

Chimmula, V. K. R., & Zhang, L. (2020). Time series forecasting of COVID-19 transmission in Canada using LSTM networks. *Chaos Solitons & Fractals, 135*. https://doi.org/10.1016/j.chaos.2020.109864

Cohen, J. E. (1992). Infectious diseases of humans: Dynamics and control. *JAMA The Journal of the American Medical Association, 268*(23), 3381.

da Cruz, N. F., Oh, D. Y., & Choumar, N. B. (2020). The metropolitan scale. *Cities, 100*. https://doi.org/10.1016/j.cities.2020.102644

Dablanc, L., Heitz, A., Buldeo Rai, H., & Diziain, D. (2022). Response to COVID-19 lockdowns from urban freight stakeholders: An analysis from three surveys in 2020 in France, and policy implications. *Transport Policy, 122*, 85–94. https://doi.org/10.1016/j.tranpol.2022.04.020

Davila, J., Uzcategui, M., & Tucci, K. (2005). A multi-agent theory for simulation, 2005 Aug 29-31. In *Paper presented at the 5th IASTED International Conference on Modelling, Simulation and Optimization, Oranjestad, Netherlands*.

Gao, Z., Wang, S., Gu, J., Gu, C., & Liu, R. (2022). A community-level study on COVID-19 transmission and policy interventions in Wuhan,China. *Cities, 127*, Article 103745. https://doi.org/10.1016/j.cities.2022.103745

Ghanim, M. S., Muley, D., & Kharbeche, M. (2022). ANN-based traffic volume prediction models in response to COVID-19 imposed measures. *Sustainable Cities and Society, 81*. https://doi.org/10.1016/j.scs.2022.103830

Ghostine, R., Gharamti, M., Hassrouny, S., & Hoteit, I. (2021). An extended SEIR model with vaccination for forecasting the COVID-19 pandemic in Saudi Arabia using an ensemble Kalman filter. *Mathematics, 9*(6). https://doi.org/10.3390/math9060636

Goenaga, B., Matini, N., Karanam, D., & Underwood, B. S. (2021). Disruption and recovery: Initial assessment of COVID-19 traffic impacts in North Carolina and Virginia. *Journal of Transportation Engineering Part A-Systems, 147*(4). https://doi.org/10.1061/jtepbs.0000518

He, S., Peng, Y., & Sun, K. (2020). SEIR modeling of the COVID-19 and its dynamics. *Nonlinear Dynamics, 101*(3), 1667–1680. https://doi.org/10.1007/s11071-020-05743-y

Hu, X., Li, L., & Dong, K. (2021). What matters for regional economic resilience amid COVID-19? Evidence from cities in Northeast China. *Cities*. , Article 103440. https://doi.org/10.1016/j.cities.2021.103440

Kandel, N., Chungong, S., Omaar, A., & Xing, J. (2020). Health security capacities in the context of COVID-19 outbreak: An analysis of International Health Regulations annual report data from 182 countries. *Lancet, 395*(10229), 1047–1053. https://doi.org/10.1016/S0140-6736(20)30553-5

Kermack, W. O., & McKendrick, A. G. (1939). Contributions to the mathematical theory of epidemics: V. Analysis of experimental epidemics of mouse-typhoid; a bacterial disease conferring incomplete immunity. *The Journal of Hygiene, 39*(3), 271–288. https://doi.org/10.1017/s0022172400011918

Kim, H., Lee, N., & Kim, S. N. (2018). Suburbia in evolution: Exploring polycentricity and suburban typologies in the Seoul metropolitan area, South Korea. *Land Use Policy, 75*, 92–101. https://doi.org/10.1016/j.landusepol.2018.03.033

Lai, S., Ruktanonchai, N. W., Zhou, L., Prosper, O., Luo, W., Floyd, J. R., & Tatem, A. J. (2020). Effect of non-pharmaceutical interventions to contain COVID-19 in China. *Nature, 585*(7825), 410–413. https://doi.org/10.1038/s41586-020-2293-x

Lai, S. J., Ruktanonchai, N. W., Zhou, L. C., Prosper, O., Luo, W., Floyd, J. R., & Tatem, A. J. (2020). Effect of non-pharmaceutical interventions to contain COVID-19 in China. *Nature, 585*(7825), 410-+. https://doi.org/10.1038/s41586-020-2293-x

Lekone, P. E., & Finkenstädt, B. F. (2006). Statistical inference in a stochastic epidemic SEIR model with control intervention: Ebola as a case study. *Biometrics, 62*(4), 1170–1177. https://doi.org/10.1111/j.1541-0420.2006.00609.x

Leontitsis, A., Senok, A., Alsheikh-Ali, A., Al Nasser, Y., Loney, T., & Alshamsi, A. (2021). SEAHIR: A specialized compartmental model for COVID-19. *International Journal of Environmental Research and Public Health, 18*(5). https://doi.org/10.3390/ijerph18052667

Li, F., Li, Y. Y., Liu, M. J., Fang, L. Q., Dean, N. E., Wong, G. W. K., & Xu, S. Q. (2021). Household transmission of SARS-CoV-2 and risk factors for susceptibility and infectivity in Wuhan: A retrospective observational study. *Lancet Infectious Diseases, 21*(5), 617–628. https://doi.org/10.1016/S1473-3099(20)30981-6Hubei430030

Liu, J., Hao, J. Y., Sun, Y. Y., & Shi, Z. W. (2021). Network analysis of population flow among major cities and its influence on COVID-19 transmission in China. *Cities, 112*. https://doi.org/10.1016/j.cities.2021.103138

Liu, J., Ong, G. P., & Pang, V. J. (2022). Modelling effectiveness of COVID-19 pandemic control policies using an area-based SEIR model with consideration of infection during interzonal travel. *Transportation Research Part A: Policy and Practice, 161*, 25–47. https://doi.org/10.1016/j.tra.2022.05.003

Liu, S., & Yamamoto, T. (2022). Role of stay-at-home requests and travel restrictions in preventing the spread of COVID-19 in Japan. *Transportation Research Part A: Policy and Practice, 159*, 1–16. https://doi.org/10.1016/j.tra.2022.03.009

Liu, Z., & Stern, R. (2021). Quantifying the traffic impacts of the COVID-19 shutdown. *Journal of Transportation Engineering Part A-Systems, 147*(5). https://doi.org/10.1061/jtepbs.0000527

Maugeri, A., Barchitta, M., Battiato, S., & Agodi, A. (2020). Estimation of unreported novel coronavirus (SARS-CoV-2) infections from reported deaths: A susceptible–exposed–infectious–recovered–dead model. *Journal of Clinical Medicine, 9*(5).

Mayer, B., & Boston, M. (2022). Residential built environment and working from home: A New Zealand perspective during COVID-19. *Cities, 129*, Article 103844. https://doi.org/10.1016/j.cities.2022.103844

Moreno-Monroy, A. I., Schiavina, M., & Veneri, P. (2021). Metropolitan areas in the world. Delineation and population trends. *Journal of Urban Economics, 125*. https://doi.org/10.1016/j.jue.2020.103242

Mphale, O., Okike, E. U., & Rafifing, N. (2022). A machine learning univariate time series model for forecasting COVID-19 confirmed cases: A pilot study in Botswana. *International Journal of Computer Science and Network Security, 22*(1), 225–233. https://doi.org/10.22937/ijcsns.2022.22.1.31

Muley, D., Ghanim, M. S., Mohammad, A., & Kharbeche, M. (2021). Quantifying the impact of COVID–19 preventive measures on traffic in the State of Qatar. *Transport Policy, 103*, 45–59. https://doi.org/10.1016/j.tranpol.2021.01.018

N. H. C. o. t. P. s. R. o.. (2020). Report of the China-WHO Joint Mission on Novel Coronavirus Pneumonia (COVID-19) released. Retrieved from http://www.nhc.gov.cn/xcs/fkdt/202002/87fd92510d094e4b9bad597608f5cc2c.shtml.

Ohmagari, N. (2022). How did the Tokyo Metropolitan Government respond to COVID-19? *Global Health & Medicine, 4*(2), 67–70. https://doi.org/10.35772/ghm.2022.01017

Pulla, P. (2020). COVID-19: India imposes lockdown for 21 days and cases rise. *BMJ-British Medical Journal, 368*. https://doi.org/10.1136/bmj.m1251

Sajadi, H., & Hartley, K. (2022). COVID-19 pandemic response in Iran: A dynamic perspective on policy capacity. *Journal of Asian Public Policy, 15*(2), 228–249. https://doi.org/10.1080/17516234.2021.1930682

Sanz, J., Xia, C. Y., Meloni, S., & Moreno, Y. (2014). Dynamics of interacting diseases. *Physical Review X, 4*(4). https://doi.org/10.1103/PhysRevX.4.041005

Shorten, C., Khoshgoftaar, T. M., & Furht, B. (2021). Deep learning applications for COVID-19. *Journal of Big Data, 8*(1). https://doi.org/10.1186/s40537-020-00392-9

Shulgin, B., Stone, L., & Agur, Z. (1998). Pulse vaccination strategy in the SIR epidemic model. *Bulletin of Mathematical Biology, 60*(6), 1123–1148. https://doi.org/10.1006/s0092-8240(98)90005-2

Takefuji, Y. (2022). Discovering COVID-19 state sustainable policies for mitigating and ending the pandemic. *Cities, 130*, Article 103865. https://doi.org/10.1016/j.cities.2022.103865

Tian, H., Liu, Y., Li, Y., Wu, C.-H., Chen, B., Kraemer, M. U. G., & Dye, C. (2020). An investigation of transmission control measures during the first 50 days of the COVID-19 epidemic in China. *Science, 368*(6491), 638-+. https://doi.org/10.1126/science.abb6105

Truong, D., & Truong, M. D. (2021). Projecting daily travel behavior by distance during the pandemic and the spread of COVID-19 infections - Are we in a closed loop scenario? *Transportation Research Interdisciplinary Perspectives, 9*, Article 100283. https://doi.org/10.1016/j.trip.2020.100283

Wang, Y., Wang, Z., Wang, J., Li, M., Wang, S., He, X., & Zhou, C. (2022). Evolution and control of the COVID-19 pandemic: A global perspective. *Cities, 130*, Article 103907. https://doi.org/10.1016/j.cities.2022.103907

Wei, Y., Wang, J., Song, W., Xiu, C., Ma, L., & Pei, T. (2021). Spread of COVID-19 in China: Analysis from a city-based epidemic and mobility model. *Cities, 110*. https://doi.org/10.1016/j.cities.2020.103010

Xiang, W., Chen, L., Peng, Q., Wang, B., & Liu, X. (2022a). How effective is a traffic control policy in blocking the spread of COVID-19? A case study of Changsha, China. *International Journal of Environmental Research and Public Health, 19*(13). https://doi.org/10.3390/ijerph19137884

Xiang, W., Chen, L., Peng, Q., Wang, B., & Liu, X. (2022b). How effective is a traffic control policy in blocking the spread of COVID-19? A case study of Changsha, China. *International Journal of Environmental Research and Public Health, 19*(13), 7884.

Xiao, Y., & Torok, M. E. (2020). Taking the right measures to control COVID-19. *Lancet Infectious Diseases, 20*(5), 523–524. https://doi.org/10.1016/s1473-3099(20)30152-3

Xiao, Y., Yang, M., Zhu, Z., Yang, H., Zhang, L., & Ghader, S. (2021). Modeling indoor-level non-pharmaceutical interventions during the COVID-19 pandemic: A pedestrian dynamics-based microscopic simulation approach. *Transport Policy, 109*, 12–23. https://doi.org/10.1016/j.tranpol.2021.05.004

Xing, G.-R., Li, M.-T., Li, L., & Sun, G.-Q. (2020). The impact of population migration on the spread of COVID-19: A case study of Guangdong Province and Hunan Province in China. *Frontiers in Physics, 8*. https://doi.org/10.3389/fphy.2020.587483

Xu, B., Gutierrez, B., Mekaru, S., Sewalk, K., Goodwin, L., Loskill, A., & Kraemer, M. U. G. (2020). Epidemiological data from the COVID-19 outbreak, real-time case information. *Scientific Data, 7*(1). https://doi.org/10.1038/s41597-020-0448-0

Yang, Z., Zeng, Z., Wang, K., Wong, S.-S., Liang, W., Zanin, M., & He, J. (2020). Modified SEIR and AI prediction of the epidemics trend of COVID-19 in China under public health interventions. *Journal of Thoracic Disease, 12*(3), 165-+. https://doi.org/10.21037/jtd.2020.02.64

Zeroual, A., Harrou, F., Dairi, A., & Sun, Y. (2020). Deep learning methods for forecasting COVID-19 time-series data: A comparative study. *Chaos Solitons & Fractals, 140*. https://doi.org/10.1016/j.chaos.2020.110121

Zhang, X., Ji, Z., Zheng, Y., Ye, X., & Li, D. (2020). Evaluating the effect of city lock-down on controlling COVID-19 propagation through deep learning and network science models. *Cities, 107*, 102869. https://doi.org/10.1016/j.cities.2020.102869